Politecnico di Torino

Corso di Laurea in Ingegneria Aerospaziale
A.A. 2020/2021
Sessione di Laurea Ottobre 2021

Reduced order modeling of blood flow

Relatore:
Prof.ssa Stefania Scarsoglio

Candidato:
Federico Vignani

SUMMARY

INTRODUCTION

Over the past few decades, reduced order models (ROMs) have been involved in a rapid development within the framework of designing and modeling complex dynamic systems, whose applications reach out in many fields, such as engineering, biochemistry, computational fluid dynamics (CFD) and so forth. The cardiovascular system, by definition a highly elaborate dynamic system constituted by an intricate network of different living vessels, is the perfect field for the application of reduced order models: many image based three dimensional models, essentials for the study of patient specific blood flow features and disease pathogenesis, have been developed aiming at achieving a better understanding of blood flow and its interaction with vessel walls. However, the intrinsic non-linearities and the vast range of spatial and time scales characterizing cardiovascular system are such that the computational burden and the numerical instability have limited the application of full-order models to clinical scenarios, due to the prohibitive costs and times of the simulations. Thus, ROMs have paved their way towards medical applications and clinical practice and can be used in conjunction with 3D models, or replace them, in order to achieve faster and less computationally expensive analysis of blood flow in physiological or pathological conditions, supporting clinicians' decisions regarding treatment and therapeutic actions.

The main purpose of this thesis is to introduce the basic concepts and theories that lay at the basis of reduced order models for the cardiovascular system and to show some applications concerning both the analysis of blood flow in vessels form a purely haemodynamic point of view and the study of pressure distribution and flow rate in arteries in pathological conditions.

The first chapter has the objective of recalling simple concepts concerning the cardiovascular system, blood flow characteristics in large arteries and some haemodynamic equations, which may be useful later in the discussion.

The second chapter starts from the concepts regarding reduced order models for blood flow highlighted in this introduction and focuses on the description of the main features and fields of application of zero dimensional and one dimensional models, then hinting at more advanced 2D and multiscale models.

Finally, in the third chapter, three applications of ROMs to the cardiovascular system and artery segments are presented. The applications are introduced in order of model dimensionality, starting with a 0D ROM and then continuing with a one dimensional and a more complex non-linear and parametrized model. The first article (*Paragraph 3.1*) aims at studying the changes in haemodynamics, especially regarding flow rate and pressure variations, at the time when acute ischemic stroke (AIS) occurs, the second is a non-clinical related 1D model (*Paragraph 3.2*) used to study the effect of different velocity profiles on the pulse wave propagation in aorta segments, while the latter (*Paragraph 3.3*) proposes a parametrized reduced order model with the objective of evaluating the severity of stenosis in the coronary artery disease.

CHAPTER 1

1.1 THE CARDIOVASCULAR SYSTEM

The cardiovascular system consists in a complex network of vessels which convey blood throughout the entire human body, in order to perform essential functions for human life, such as transporting nutrients and oxygen to tissues and organs, removing waste products like CO_2, regulating pH, body temperature and the level of hormones present within blood [1]. The focal point of the cardiovascular system is of course the heart, an automatically-regulated muscular organ divided in four chambers (two atria and two ventricles) that acts as a pump to vehicle blood across the vessels to specific and precise destinations, under the action of electrical stimuli, which lead to the contraction and relaxation of the heart itself.

The sequence of cardiac events during a normal heartbeat is defined as cardiac cycle: first atria contract and ventricles are relaxed, then ventricles contract and atria are relaxed, finally atria and ventricles are both relaxed. The contraction phase is called systole, while the relaxation phase is called diastole.

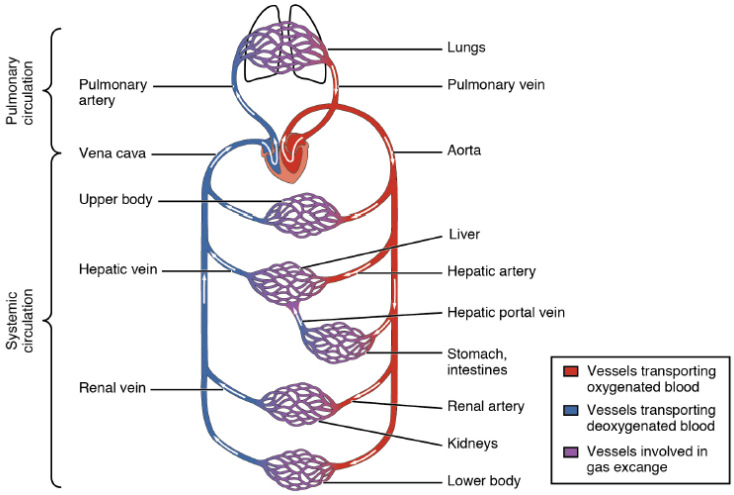

Figure 1: simplified structure of the cardiovascular circulation; pulmonary and systemic circulation. [8]

For ease, the cardiovascular system can be divided into two main circuits (*Figure 1*): the pulmonary and systemic circulation (respectively PC and SC in abbreviated form). The first has the task of bringing oxygenated blood from the alveoli, located inside the lungs, to the left side of the heart through a series of vessels that increase dimensions and thickness at the time that blood is approaching to the heart (first venules, then two pulmonary veins), while deoxygenated blood is carried the opposite way, from the right side of the heart towards the lungs (blood leave the heart through the pulmonary artery and then convey in arterioles and capillaries, forming a tree-like structure). On the other hand, SC carries oxygenated blood from the left heart side throughout the whole body in order to supply organs and tissues (the main artery of the systemic circuit is the aorta), while deoxygenated blood is returned to the right heart side by a series of veins, which culminate in the vena cava [1].

That being said, it is clear that arteries vehicle blood full of oxygen from the heart to the periphery of the body, while veins carry the carbon dioxide full fluid in the opposite sense, from the organs and tissues, where exchanges take place through capillaries, to the so called engine of the cardiovascular system. This difference in function is also reflected into the physical and structural difference that distinguish arteries from veins: by focusing just on SC, the mean pressure is much higher in arteries than in veins (the difference is around 85 mmHg), as well as the vessel wall thickness (arteries large for SC, veins small) and finally, in veins there are valves located along the limbs which are absent in arteries [2]. Arterial pressure is pulsatile, while arteriolar, venular and venous blood pressure are weakly pulsatile/almost constant.

As stated by C.M. Colciago et al. in [3], far from being inert pipes that convey the blood to organs of the body, arterial vessels are complex living tissues with locally-variable elastic and viscoelastic mechanical properties, that can interact with blood flow and adapt to certain conditions depending on several factors, thus causing changes in the geometries and physical properties of the vessels (for example, it has been shown that lifestyle, genetics and age have an impact on this features). The next paragraph will focus on blood dynamics related to arterial vessels, as venous blood flow is neglected for the sake of the discussion.

1.2 BLOOD AND HAEMODYNAMICS

Blood is the fluid that flows inside the cardiovascular system pumped by the heart towards organs and tissues, in order to carry out essential metabolic functions. As far as haemodynamic is concerned, blood can be defined as a viscous and inhomogeneous fluid, characterized by corpuscular elements aggregating or separating in specific conditions, that give an inconstant contribution to the fluid dynamic response of the cardiovascular system [1]. Blood viscosity is not fixed and varies depending on the vessel dimension and flow rate (circulation can be characterized by three types of flows, namely laminar in arteries, arterioles and veins, turbulent in the left ventricle and single file flow in capillaries [4]). The fact that blood viscosity is variable with shear rate makes this fluid non-Newtonian: even if at low shear rate, blood shows a non-Newtonian behaviour (particles tend to form aggregates), nevertheless, in large arteries with diameter larger than 0.3 cm, it is widely accepted to assume a Newtonian behaviour [5].

Furthermore, arterial pressure and flow rate are pulsatile, unsteady, thus the interaction between blood flow and the vessel wall gives rise to mechanical stimuli such as stress exchange and, with time, can also lead to a reduction in the resistance to fatigue of the elastic fibres [3]; these are important risk factors that have to be kept in mind when modelling the cardiovascular system. Indeed, some studies have highlighted that friction forces related to viscosity, despite being much smaller in intensity than pressure, play a significant role in the development of atherosclerosis [7].

Focusing back on the pulsatile nature of arterial pressure, the latter ranges from diastolic pressure value to systolic value, however, maximum and minimum levels, as much as pressure waveforms, vary with the distance from the heart (*Figure 2*): moving away from the heart, pressure signals delay (due to arterial walls elasticity and fluid dynamic nonlinearities) and increase in amplitude, propagating as a wave at finite speed (pulse wave speed) [8].

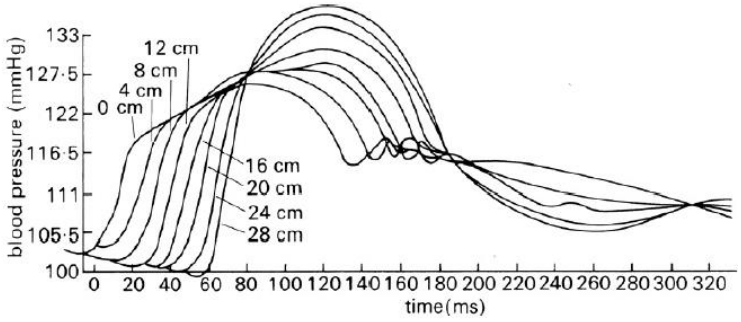

Figure 2: pressure waveforms at multiple sites at the same time along a canine aorta. [8]

Moreover, it is clear that arteries lack of uniformity in both geometrical and mechanical properties, thus, at each discontinuity site along the vessels, pulse wave is partially reflected, which causes asynchrony between aortic pressure and flow rate in systole [8]. Pulse wave transmission and reflection phenomena can be studied through 1D reduced order models (see *Paragraph 2.3*).

Dealing with blood flow in arteries, where it is accepted the hypothesis of laminar flow and Newtonian fluid, the resistance opposed by the vessel wall to the stream can be estimated considering Poiseuille's law:

$$\Delta Q = \frac{\pi \Delta_p r_v^4}{8 \mu l_v} \qquad (1)$$

where ΔQ is the mean flow rate, Δ_p the pressure drop, r_v and l_v are the tube radius and length, respectively, and μ is the fluid viscosity. Poiseuille's law can also be rewritten as follows:

$$\Delta_p = R\, \Delta Q \qquad (2)$$

being R the hydraulic resistance. In terms of an electric-hydraulic analogy, Poiseuille's law in fluid dynamics can be seen as Ohm's law for electrical circuits. Although Poiseuille's law hypothesis are not satisfied in general, being blood non-Newtonian, pulsatile and developing not in perfect cylindrical tubes, it can still be applied to approximate blood stream in arteries [6] and can be used in 0D models for blood flow (see *Paragraph 2.2*).

1.3 NAVIER-STOKES EQUATIONS

As well as other fluid systems, blood flow in the cardiovascular system complies with the laws of mass conservation and momentum balance, derived from the formulation of unsteady Navier-Stokes equations, which establish a connection between the main parameters of a moving fluid, such as pressure, density and velocity. Given an open bounded domain, unsteady Navier-Stokes equations for a Newtonian and incompressible fluid read as follows [9]:

$$\begin{cases} \nabla \cdot \vec{u} = 0 \\ \rho \dfrac{\partial \vec{u}}{\partial t} + \vec{u} \cdot \nabla \vec{u} = -\nabla p + \mu \nabla^2 \vec{u} + \rho \vec{g} \end{cases} \tag{3}$$

Being $\vec{u}$ the velocity vector, ρ blood density, μ blood dynamic viscosity and $\vec{g}$ the g-force vector.

Approximately, an arterial vessel can be considered as a cylinder, although it has been already said that vessels are flexible and can interact with blood flow by altering their geometry (this implies the necessity of additional boundary conditions that strongly influence the blood flow dynamic [10]); in cylindrical coordinates, being $\vec{u} = u_r \vec{e}_r + u_\theta \vec{e}_\theta + u_z \vec{e}_z$, Navier-Stokes equations can be written in the form:

$$\frac{1}{r}\frac{\partial}{\partial r}(r u_r) + \frac{1}{r}\frac{\partial u_\theta}{\partial \theta} + \frac{\partial u_z}{\partial z} = 0 \, ;$$

$$\frac{\partial u_r}{\partial t} + u_r \frac{\partial u_r}{\partial r} + \frac{u_\theta}{r}\frac{\partial u_r}{\partial \theta} - \frac{u_\theta^2}{r} + u_z \frac{\partial u_r}{\partial z} = -\frac{1}{\rho}\frac{\partial p}{\partial r} + \nu\left(\nabla^2 u_r - \frac{u_r}{r^2} - \frac{2}{r^2}\frac{\partial u_\theta}{\partial \theta}\right) + g_r \, ;$$

$$\frac{\partial u_\theta}{\partial t} + u_r \frac{\partial u_\theta}{\partial r} + \frac{u_\theta}{r}\frac{\partial u_\theta}{\partial \theta} + \frac{u_\theta u_r}{r} + u_z \frac{\partial u_\theta}{\partial z} = -\frac{1}{\rho r}\frac{\partial p}{\partial \theta} + \nu\left(\nabla^2 u_\theta - \frac{u_\theta}{r^2} + \frac{2}{r}\frac{\partial u_r}{\partial \theta}\right) + g_\theta \, ; \tag{4}$$

$$\frac{\partial u_z}{\partial t} + u_r \frac{\partial u_z}{\partial r} + \frac{u_\theta}{r}\frac{\partial u_z}{\partial \theta} + u_z \frac{\partial u_z}{\partial z} = -\frac{1}{\rho}\frac{\partial p}{\partial z} + \nu \nabla^2 u_z + g_z \, ;$$

As far as reduced order models are concerned (see *Chapter 2* for ROMs), solutions for Navier-Stokes equations can be obtained only for simple geometries and non-complicated axisymmetric domains; for example, assuming an 1D blood flow field along the direction z, Navier-Stokes equation system previously written reads as

$$\begin{cases} \dfrac{\partial u_z}{\partial z} = 0 \, ; \\ \dfrac{\partial u_z}{\partial t} + u_z \dfrac{\partial u_z}{\partial r} = -\dfrac{1}{\rho}\dfrac{\partial p}{\partial z} + \nu\left[\dfrac{1}{r}\dfrac{\partial}{\partial r}\left(r \dfrac{\partial u_z}{\partial r}\right)\right] + g_z \, ; \end{cases} \tag{5}$$

CHAPTER 2

2.1 REDUCED ORDER MODELS (ROMs) FOR THE CARDIOVASCULAR SYSTEM

Nowadays, when approaching the study of complex phenomena and the analysis of dynamical systems, modelling and numerical simulations have become crucial tools for the control and design of parametrized systems [11]. Unfortunately, especially in the field of computational fluid dynamics, the nonlinearities intrinsically present in the systems, the uncertainty affecting the values of the parameters and the wide range of spatial and time scales makes the simulation of a full-order model (FOM) extremely expensive in terms of computational cost (e.g. simulations regarding blood flow through the heart chambers require the solution of systems of partial differential equations (PDEs) with up to 10^6 degrees of freedom, which can take several hours of simulation [12]; advanced computing architectures are also needed).

The limitations highlighted in the simulation of full-order models lead to the necessity of finding new data-driven techniques in order to develop lower-order models which can be used in conjunction with FOMs: in this way, faster and cheaper analysis can be performed, preserving the most important features of the FOM without sacrificing the accuracy of the general physical behaviour of the analysed system [13].

Therefore, reduced order models (ROMs) allow to decrease the computational burden derived from FOMs, providing reliable, accurate and fast numerical simulations. More than for other branches of engineering and applied sciences, performing accurate computations in a short amount of time, minutes, rather than hours, or even days, is crucial when dealing with problems arising from life sciences, like, for example, in the simulation of the cardiovascular system [12].

It is no wonder that the numerical modelling of the cardiovascular system based on reduced order models has experienced a strong development in recent years and is now becoming a paradigm in healthcare technology, not only due to the physical and geometrical complexity of the subject, but, above all, it has paved the way for clinical application, aiming at shedding light on the pathogenesis of cardiac and vascular diseases [14] and overcoming the main limitations of in-vivo studies, which are typically invasive, expensive and not easy to carry out [15]. Moreover, numerical simulations can study the behaviours of quantities which cannot be measured directly, such as the wall shear stress [12] on vessels lumen, a factor often linked to pathologies like atherosclerosis and thrombogenesis. This is meant to enable quantitative analysis in several virtual scenarios in order to support clinicians' decisions and to enhance diagnostic practices based on medical imaging [12].

Over the past several years, many researchers have developed numerous and different models for the designing of the cardiovascular system, answering both clinical and fluid dynamic questions. The types of ROM vary depending on the final aim, the accuracy and reliability required and on the field of application, ranging from zero dimensional to three dimensional and multiscale models. In the following pages, some basic concepts are given regarding 0D, 1D, 2D and multiscale models, highlighting the main themes and fields of application, while in the next chapter (*Chapter 3*), applications of ROMs to case studies regarding blood flow in arteries are presented.

2.2 0D MODELS FOR THE CARDIOVASCULAR SYSTEM

Zero dimensional models (0D), also referred to as lumped parameter models (LPM or LP), are simplified models developed to simulate the global haemodynamics of the whole circulation system: the main physical variables and parameters, such as flow rate, pressure and volume are supposed to have a uniform distribution at any time within each cardiovascular domain (vessels, organs and so on) [10]. Thus, the model resolution involves just a set of ordinary differential equations (ODEs), much more simply solvable than systems of PDEs arising from full-order models.

As thoroughly explained by Shi et al. [10], in the context of 0D modelling, a hydraulic-electric analogy subsists: hydraulic impedance represents the combined effect of the frictional loss, vessel wall elasticity and blood inertia in the blood flow, whilst electric impedance represents the combination of the resistance, capacitance and inductance in the circuit. Moreover, blood flow is described by the continuity equation for mass conservation, Poiseuille's Law for the steady state momentum equilibrium (see *Paragraph 1.1*), and the Navier-Stokes equation for the unsteady state momentum balance; similarly the electric flow in the circuit is governed by the Kirchhoff's current law for current balance, and Ohm's law for the steady state voltage-current relation. Thus, by representing the blood pressure and flow-rate with voltage and current, describing the effects of friction and inertia in blood flow and of vessel elasticity with resistance R, inductance L and capacitance C (related to storage properties of arteries) in the electric circuit respectively, the well-established methods for analysis of electric circuits can be borrowed and applied to the investigation of cardiovascular dynamics [10].

Although widely spread and utilized and characterized by a low computational cost, 0D models neglect peculiar aspects of haemodynamics, such as the propagation and reflection of pressure and flow waves, thus being unable to simulate the effect of high frequency components in the arterial impedance (venous pressure is also set to zero) [10].

The first model for the cardiovascular system which is considered the precursor of 0D models, also known as the two-elements Windkessel model (*Figure 3a*), was introduced by Otto Frank in [16]: it represents the systemic arterial tree by means of a resistance and a compliance (the resistance stands for the dissipative nature of vessels, while the compliance reveals the storage properties of large arteries).

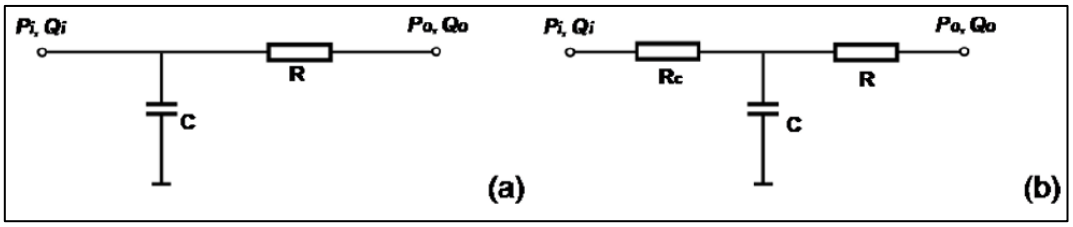

Figure 3: (a) RC Windkessel model; (b) RCR Westkessel model. [10]

The model well describes the decay of the systemic arterial pressure during diastole, but fails at reproducing what happens during systole, due to pressure's high frequencies. Later on, many models were developed starting from the Windkessel circuit, e.g. the Westkessel model (*Figure 3b*) by Westerhof et al., which introduces another resistance in order to clarify the behaviour of blood

flow at high frequencies (these models are called mono-compartment models, as they represent the cardiovascular system as a unique block, while multiple compartment ones consider the global circulation as divided in various defined regions with peculiar properties).
0D models are currently widely applied in various areas of cardiovascular studies, ranging from basic cardiovascular physiology research to astronautic medicine and design of artificial organs [10]; furthermore, zero dimensional models are used for the representation of the contractility of heart chambers, the functioning of the cardiac and venous valves, the distal coronary districts and for the simulation of Acute Ischemic Stroke [17].

2.3 1D MODELS FOR THE CARDIOVASCULAR SYSTEM

Unlike 0D models, which neglect some important haemodynamic aspects, one-dimensional models enable to inquire into the propagation and reflection phenomena of pressure and flow rate waveforms [8], thus permitting the numerical study of the systemic arterial tree. Therefore, 1D ROMs for blood flow analysis in arterial vessels typically rely on a time domain based one-dimensional wave propagation model, which can include the nonlinear convective acceleration term or not, depending on the purpose of the simulations. In general, one-dimensional models are derived from a reduced and simplified axisymmetric version of the Navier-Stokes equations (see *Paragraph 1.3*), generating a system of hyperbolic PDEs often accompanied by specific boundary conditions and other algebraic relations. Basically, nearly all 1D model proposed for the study of pulse wave transmission in arterial vessels are based on a similar derivation and the differences among these models are mostly in the boundary conditions applied and in the solution methods used, and whether nonlinear effects are considered for the different applications [10]. Another difference between these models concerns the artery vessel wall modeling, which can be implemented using a linear elastic or a linear viscoelastic material model. Various cross-sectional velocity profiles can be used to evaluate the nonlinear convection and diffusion terms present in the momentum equation of blood flow [18] (a modified flat velocity profile was used by Formaggia et al. [19], Steele et al. [20] resorted to a Poiseuille velocity profile, while Bessems et al. [21] proposed an approximate logarithmic velocity profile).

Moreover, 1D models are usually formulated using flow rate, cross-sectional area of artery and pressure as the main variables and are solved numerically in time and space with a low computational cost compared to full-order models simulations. However, there are several complications in the study of one-dimensional pulse wave propagation, including the tapering of the vessel, which cause rapid variations in convective acceleration, vessel branching, nonlinear pressure/cross-sectional area relationships for the vessel wall and bending in the vessel wall itself [10]. Therefore, boundary conditions must be applied: the resolution of a 1D model for pulse wave transmission typically requires the imposition of three types of boundary conditions, one to each end of the considered vessel segment and one at each arterial junction (arteries are branched and connected to smaller arterioles, so it is impossible to trace all the vessel branching in the simulation and the model must be terminated at some point, depending on the specific aim of the study [10]). The boundary conditions at arterial bifurcations usually consist in the conservation of mass and total pressure, while at the upstream side of the vessel the conditions consist in periodic signals of the dependent variables [8] or can be derived from experimental data. As far as downstream conditions are concerned, in more recent studies has become popular the use of a simple or

otherwise non-complex 0D model, such as a two-element (RC) or three-element (RCR) Windkessel model, in order to clarify the pressure/flow relation at the outlet of the vessel [10].

As previously mentioned, the principal application of one-dimensional models concerns the study of pulse wave transmission within arterial vessels and the differences among these models mainly consist in the choice of domain, wall mechanical properties, velocity profile, boundary conditions and numerical methods [8].

2.4 2D AND MULTI-SCALE MODELS FOR THE CARDIOVASCULAR SYSTEM

Two dimensional models (2D) are obviously mostly based on the Navier-Stokes equations, which are strongly non-linear partial differential equations whose behaviour may be parabolic, hyperbolic or elliptic, depending on the nature of the problem studied [10]. Compared to 0D and 1D models, bi-dimensional ROMs consent to carry out more precise calculations of the pressure and flow fields in axisymmetric arterial vessels, although implying a higher computational burden, therefore are often applied for the analysis of small cardiovascular regions (coronary arteries, cardiac valves or small segments of vessels in presence of stenosis or other pathological conditions). Many models have been proposed in order to achieve a low-dimensional parametrization of the complex computational domain of the Navier-Stokes equations, creating for example reduced base (RB) constructions relying on the Proper Orthogonal Decomposition (POD) method. The main aim is to cross-sectionally average the Navier-Stokes equations to obtain 2D or quasi-1D PDEs equations, obviously more computationally expensive than ODEs and usually more prone to numerical stability [22].

As stated by Shi et al. [10], the cardiovascular system is a closed network in which subsist strong interactions between its components, therefore, the mere application of a single reduced order model like 0D for describing the global circulation dynamics, 1D or 2D for studies on local flow features, is not sufficient in order to obtain full information on vascular response. In order to address the requirement of high accuracy and ability to simulate the interaction among cardiovascular organs [10], multi-scale models are developed by coupling different ROMs, thus managing to represent in a more complete way the cardiovascular system and blood flow. To create a multiscale mathematical model of blood flow is sufficient to combine at least two models of different dimensions (the most frequently employed models are 0D and 1D, whose union can provide boundary conditions for advanced 3D or full-order models); although the fundamental utility of multi-scale models, with the increasing of the number of single ROMs jointed, a problem concerning the stability of this method arises: in the solution of multi-scale problems, generally the single scale models are still calculated as they were in the independent studies, whilst at the interfaces special care is required in the handling of the boundary conditions to ensure that the problem is well-posed in the mathematical sense. Because the blood flow in most physiological/pathological conditions is subcritical, one boundary condition needs to be set for each side of every multi-scale model considered [10]. This obviously increase the complexity of the model development.

CHAPTER 3

In this chapter, some applications of reduced order models of blood flow and cardiovascular system are shown, starting from a 0D model and then focusing on a 1D and a parametrized reduced order model.

3.1 APPLICATION OF A LUMPED PARAMETER MODEL (0D) FOR THE SIMULATION OF ACUTE ISCHEMIC STROKE (AIS)

Acute ischemic stroke (AIS) is defined as the acute condition of occlusion of a cerebral artery and since blood can flow no more through that artery, a region of the brain suffers of blood perfusion loss. One of the main risk factors related to AIS is considered to be a Hypertensive Condition (HC), that is to say a chronic situation in which systolic blood pressure exceeds the value of 130-140 mmHg depending on age, sex, smoke, weight and personal health [17]. HC on long terms leads to a modification in arterial radius, vessel thickness, Young modulus and thus changes vessel impedance [23]. Due to its sudden occurrence, AIS is not observable the right moment it occurs, so information about instantaneous changes in hemodynamics is limited. Hemodynamic instantaneous changes in occluded human arteries when AIS takes place are quantitatively assessable only via animal models or, in the last decade, via computational models [17].

An integrated 0D, or Lumped Parameter model, from now on abbreviated as LP, of the cardiovascular system with the aim of simulating an AIS and describing instantaneous changes in haemodynamics has been proposed by L. Civilla et al. in [17]: as stated by the authors, “LP models may be suitable to describe the cardiovascular system during AIS, in which the time window of interest is limited to the very first seconds after the occlusion, and thus wave reflection and transmission effects are not considered”. Regarding the simulations, three different regimens, namely physiological, HC and AIS regimen, have been considered.

In the integrated LP model of the cardiovascular system, heart chambers have been modelled with elastance systems with controlled pressure inputs, heart valves have been modelled with static binary (open/closed) pressure-controlled valves and eventually, the vasculature has been modelled with resistor-inductor-capacitor (RLC) direct circuits and have been linked to the rest of the system through a series connection (viscous resistance, fluid inertance and vessel wall elasticity have been taken into account). After simulating physiological conditions, HC has been simulated by changing pressure inputs and constant RLC parameters. Then, AIS occurring in arteries of different sizes have been simulated by considering time-dependent RLC parameters due to the elimination from the model of the occluding artery; instantaneous changes in hemodynamics have been evaluated by Systemic Arteriolar Flow (Q_a) and Systemic Arteriolar Pressure (P_a) drop with respect to those measured in HC [17].

3.1.1 MODEL IMPLEMENTATION

As mentioned above, the integrated Lumped Parameter model of the cardiovascular system developed by Civilla et al [17] includes four heart chambers, as well as four heart valves, both

described by simple governing equations, such as mass conservation and relations for pressure P and flow Q through the valves and chambers, and Systemic Circulation (SC) and Pulmonary Circulation, implemented as a direct resistor-inductor-capacitor (RLC) circuit that takes into account vessel viscous resistance, fluid inertance and vessel wall elasticity. Moreover, large arteries have been modelled with RLC circuits, while arterioles/capillaries with a simple resistor and, finally, veins with RC circuits.

Subsequently, the LP model has been implemented in a closed-loop electrical circuit in MATLAB SIMULINK R2019b (*Figure 4a*) and the Simscape Electrical™ package has been used to implement the electrical analogue.

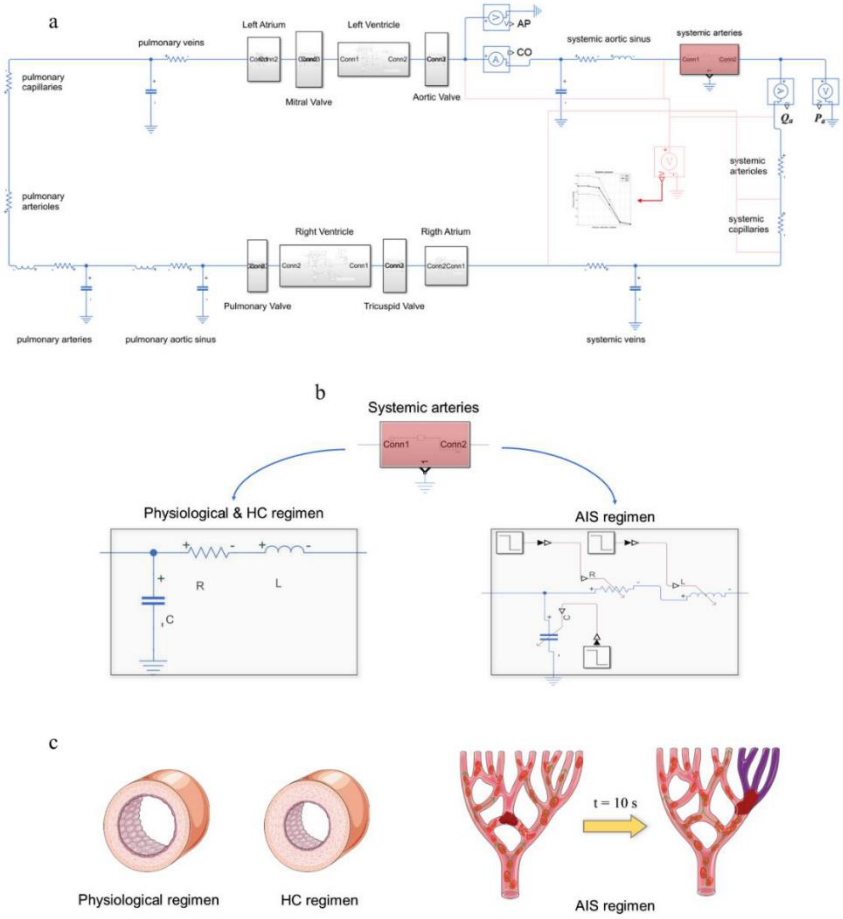

Figure 4: a) SIMULINK implementation of the integrated lumped parameter model of the cardiovascular system. Heart chambers and valves in grey boxes, vessels are represented with their extended electrical analogue apart from systemic arteries (red box). Current and voltage sensors have been inserted to measure flows and pressures downstream to the aortic valve and systemic arteries; net of voltage measurements has been implemented (in red) to measure pressures downstream to systemic components. b) Implementation of systemic arteries for physiological and hypertensive condition regimens and for the acute ischemic stroke regimen. c) Anatomical representation of the vascular situation (reproduced from Servier smart medical art) [17].

Model implementation has been obtained by linking in series heart chambers, valves, SC and PC [17]. Clearly, the modelling of systemic arteries and the values of the main parameters and input data varies depending on the regimen under which the simulations are conducted (physiological, HC or AIS): for physiological and HC regimens, systemic arteries consist in RLC circuits, but the constant parameters used are different, while for AIS, RLC circuits are based on time dependant parameters. As stated by Civilla et al. [17], parameter values for physiological conditions were taken from the study led by Korakianitis et al. [24] and values for HC and AIS regimens were derived based on an analogy between humans and rats, describing R, L and C elements with the following equations:

$$R = \frac{8\,l\,\mu}{\pi\,r^4}\ ;\ L = \frac{9\,l\,\rho}{4\,A}\ ;\ C = \frac{3\,l\,\pi\,r^3}{2\,E\,h} \qquad (6)$$

in which l is the length of the lumped artery/vein, r is its radius, E is its elastic modulus, h is its thickness, A is the cross section, μ is the kinematic viscosity of blood, considered as $4 \cdot 10^{-3}$ (Pa·s), and ρ is blood density, considered constant and equal to 1060 (kg/m^3) [17]. According to Civilla et al. [17], the length of the occluding artery l is the parameter that most influences anatomical variability with respect to internal radius, vessel wall thickness and parameters present in the equations previously written. As such, length l has been assumed as the main parameter able to determine the gravity of an AIS.

In their study, Civilla et al. [17] considered a series of ten occluding independent arteries (A_1-A_{10}), whose different lengths were assumed based on the anatomical values derived from precedent studies and simulated blood flow within the arteries in all the three regimens, focusing closely on the differences in haemodynamics during the transition from HC conditions to AIS regimen. The following table (*Table 1*) shows the values used during the simulations of the main parameters of the ten arteries in AIS regimen, namely length (l), radius (r), thickness (h), elastic modulus (E) and R, L, C values calculated with the equations mentioned above:

Occluding artery	*l* *cm*	*r* *cm*	*h* *cm*	*E* *10^4 mmHg*	*R* *mmHg·s/ml*	*L* *mmHg·s^2/ml*	*C* *10^{-3} ml/mmHg*
A_1	0.5	0.1	0.03	1.2	0.382	2.848	0.007
A_2	1.0	0.1	0.03	1.2	0.764	5.697	0.013
A_3	2.0	0.1	0.03	1.2	1.529	11.393	0.026
A_4	5.0	0.1	0.03	1.2	3.822	28.483	0.065
A_5	8.0	0.1	0.03	1.2	6.115	45.573	0.105
A_6	10.0	0.1	0.03	1.2	7.643	56.967	0.131
A_7	12.0	0.1	0.03	1.2	9.172	68.359	0.157
A_8	14.0	0.1	0.03	1.2	10.701	79.753	0.183
A_9	17.0	0.1	0.03	1.2	12.994	96.843	0.222
A_{10}	20.0	0.1	0.03	1.2	15.287	113.933	0.262

Table 1: values for model parameters for AIS regimens, considering ten different occluding arteries. [17]

3.1.2 SIMULATIONS AND RESULTS

After conducting the simulation of the physiological conditions during 5000 cardiac cycles, simulations of HC and AIS took place and lasted 20 s (10 for one and for the other regimen); as stated by Civilla et al. [17], change from HC to AIS regimen has been simulated as an instantaneous event and change in model parameters values has been simulated with a step function at time equal to 10 s. For both physiological and HC regimens, Aortic Pressure (AP) and Cardiac Output (CO) have been computed at the outlet of the aortic valve by means of a voltage and a current sensor. Systemic Arteriolar Flow (Q_a) and Systemic Arteriolar Pressure (P_a) are assumed as output of the model, and the difference between Q_a at HC at the last peak before AIS occurrence and Q_a at the first peak after AIS occurrence has been indicated as ΔQ_a. Analogously, the difference between P_a at HC at the last peak before AIS occurrence and P_a at the first peak after AIS occurrence has been indicated as ΔP_a. The values of Q_a and P_a have been measured only in AIS regimen with current and voltage sensors downstream with respect to systemic arteries. Those measurements were then used to compute ΔQ_a and ΔP_a [17]. The values of ΔQ_a and ΔP_a obtained after the simulation are listed in *Table 2* for all ten arteries A_1-A_{10}.

Occluding artery	ΔQ_a *ml/s*	ΔP_a *mmHg*
A_1	1.93	1.98
A_2	0.87	0.89
A_3	0.42	0.42
A_4	0.16	0.16
A_5	0.10	0.10
A_6	0.08	0.08
A_7	0.07	0.07
A_8	0.06	0.06
A_9	0.05	0.05
A_{10}	0.04	0.04

Table 2: variation in Systemic Arteriolar Flow (ΔQ_a) and Systemic Arteriolar Pressure (ΔP_a) for the considered ten occluding arteries. [17]

The simulation carried out by Civilla et al. [17] allows to compare the values of systolic, diastolic and mean blood pressure in physiological, HC and AIS conditions, as well as Aortic Pressure (AP) and Cardiac Output (CO). As explained by the authors, the values of systolic and diastolic blood pressure get closer to the mean value as smaller vessels are considered, following a physiological trend, as it is shown in *Figure 5*, while AP and CO in HC are higher than those in the physiological regimen (*Figure 6*).

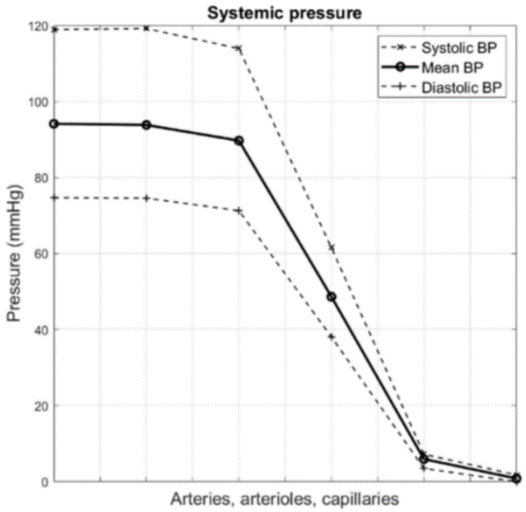

Figure 5: Systolic, diastolic and mean BP measured for every element of the systemic circulation for the physiological regimen

Cardiac output at closed valve is maintained at 0 ml/s per cycle in both physiological and HC regimens; the peak it reaches in physiological regimen is 980.50 ml/s, while in HC it is higher and reaches 1049.70 ml/s. In physiological condition, systolic and diastolic AP reach 118.90 mmHg and 76.30 mmHg respectively; in HC systolic and diastolic AP reach 137.90 mmHg and 87.70 mmHg, respectively [17].

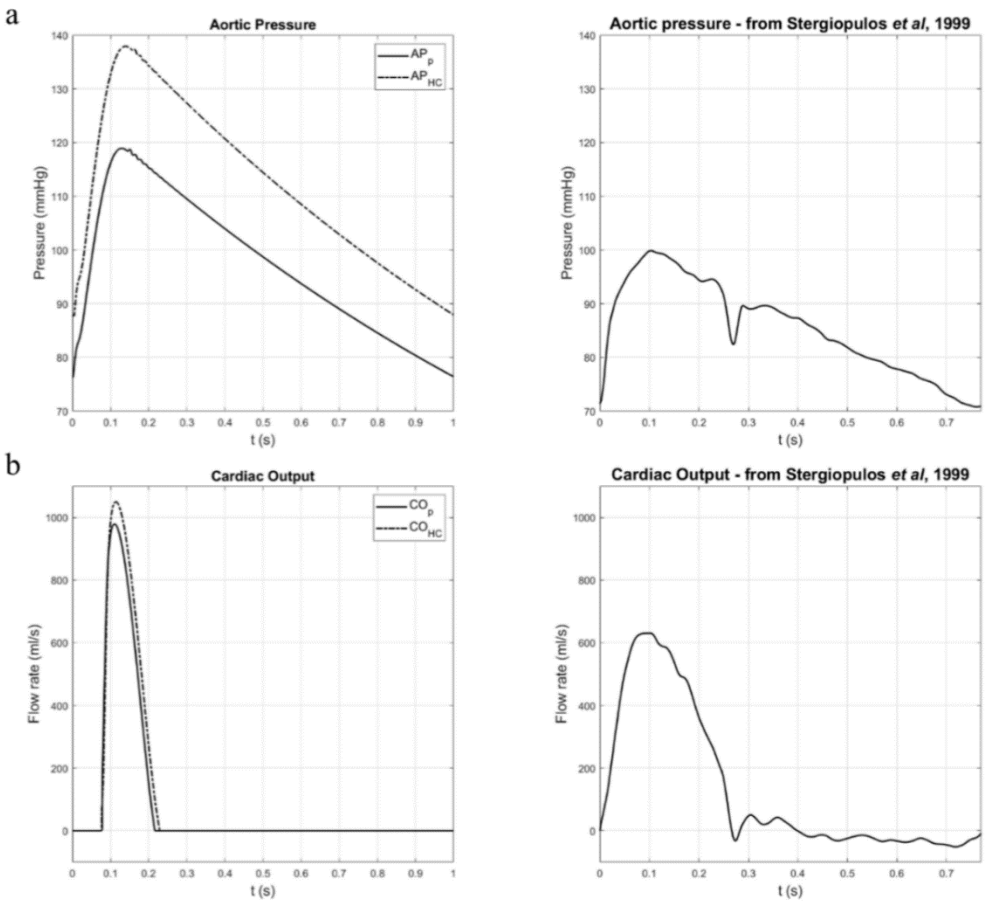

Figure 6: Aortic pressure (a) and Cardiac output (b) for the physiological (AP_P and CO_P) and the hypertensive condition regimens (AP_{HC} and CO_{HC}) compared with the experimental trends proposed by Stergiopulos et al. [25]

Moreover, by reference to *Table 2*, it is shown that the average ΔQ_a after the ischemia is 0.38 ml/s per cycle, with maximum and minimum variations respectively of 0.04 ml/s and 1.93 ml/s. These values correspond to a 0.3% loss in Q_a peak from before to after occlusion. For P_a the results are similar, with a mean value of variation of 0.39 mmHg per cycle and minimum and maximum variations of 0.04 mmHg and 1.98 mmHg per cycle. When considering only arteries shorter than 10 cm, the average loss for Q_a and P_a is respectively of 0.59 ml/s and 0.61 mmHg per cycle, this one corresponding to 0.5% of the simulated hypertensive peak [17].

The small dimensions of the occluding artery during AIS lead to a small loss of Q_a and P_a with respect to the HC regimen, thus these results highlight that it is so hard to detect an AIS simply by measuring drops of pressure or blood flow. Basically, the results about the magnitude of ΔQ_a and ΔP_a point out the difficulty of experimentally evaluate hemodynamics when an AIS occurs [17]. As regards to the results obtained in the physiological regimen in terms of systolic, diastolic and mean blood pressure, these are coherent with real values and with data extrapolated from literature. In particular, *Figure 6a* shows that the aortic pressure curve is more or less close to the one derived from the study of Stergiopulos et al. [25], although lacking the characteristic dicrotic notch and some oscillations; instead, the trend of CO is slightly different in shape (*Figure 6b*) since it does not replicate the retrograde incision in flow, being the motion of the valves modelled as instantaneous; moreover, the peak value of CO obtained with simulation is higher than the experimental value, probably due to flow velocity reduction from aortic valve to the ascending aorta, where the pressure has been measured [25]. In the HC regimen, the higher systolic blood pressure implies a higher CO (this value can be affected by errors within parameter data, being based on assumptions derived from animal models, as stated in *Paragraph 3.1.1*).

The fact that hemodynamic variations due to AIS resulted from the lumped parameter model introduced by Civilla et al. [17] are very small with respect to HC, surely underlines the difficulty of spotting major instantaneous changes in blood flow when AIS occurs just by focusing on the pressure and flow drop. However, as stated by Civilla et al. [17], a correlation can be highlighted between the length of the occluding artery and the inverse of arteriolar pressure drop: a linear regression analysis has been performed in [17] between the reciprocal of ΔQ_a and the length of the occluding artery, l (the same has been conducted with ΔP_a^{-1} and l). The results are shown in *Figure 7*. Shorter arteries lead to higher drops in arteriolar pressure, but since their magnitude is very low, the reliability of the linear regression has to be verified with further studies. In fact, a longer occluding artery leaves more cells without perfusion than a smaller one, making more damages. That could be used to link the severity of AIS to the length of the occluded artery [17].

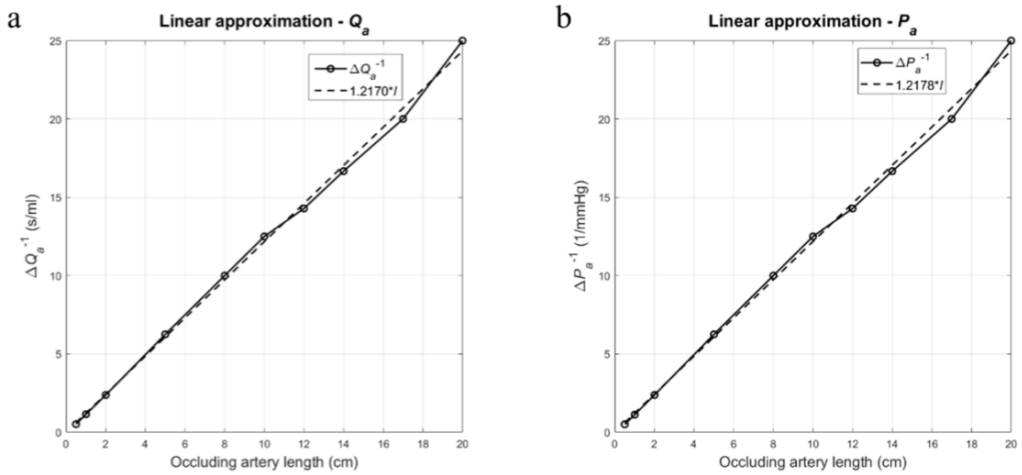

Figure 7: association of ΔQ_a (a) and ΔP_a (b) with the length of the occluding artery. [17]

3.2 APPLICATION OF 1D MODEL FOR THE STUDY OF BLOOD FLOW IN ARTERIES WITH THREE DIFFERENT CROSS-SECTIONAL VELOCITY PROFILES

As previously mentioned in *Paragraph 2.3*, one dimensional models have been used for many decades to study arterial hemodynamics due to their relative ease of application to a larger arterial network and ability to supply more accurate boundary condition to the higher dimensional models [18]. Moreover, as opposed to 0D models, one dimensional ones are suitable to study pulse wave propagation through arterial network, thus giving a better understanding on haemodynamics and disease pathogenesis.

This section will now focus on the study led by Hasan et al. [18], concerning the modeling of a single artery and arterial network with a 1D ROM, which considers three different cross-sectional velocity profiles used in the calculation of the nonlinear convective force and the frictional force, namely modified flat, parabolic and the one derived from the work of Bessems et al. in [21]. Clearly, blood flow behaviour in a single artery and in arterial network has been studied using a time domain based one-dimensional wave propagation model, derived from 1D axisymmetric Navier-Stokes equations; furthermore, the mechanical behaviour of arterial walls was approximated by means of both linear elastic and linear viscoelastic material models. Numerical simulations and analysis are carried out in two separate cases, the first considering a single and isolated artery (aorta), while the latter studies pressure and flow rate variations due to the three velocity profiles within aorta, idealized as an arterial network composed by 20 small and large size arteries and branches.

Therefore, in summary, as stated by Hasan et al. [18], the present study is aimed at investigating the effect of approximate cross-sectional velocity profile functions (modified flat, parabolic and logarithmic, proposed by Bessems [21]) on the flow characteristics for elastic and viscoelastic arterial wall constitutive laws [18].

3.2.1 MODEL IMPLEMENTATION

The one dimensional wave propagation model considers blood flow along the axial direction with constant pressure across a cross-section of the artery; the 1D Navier-Stokes equations describing the wave propagation of a laminar, axisymmetric, incompressible and fully developed flow read as follow [18]:

$$\frac{\partial A}{\partial t} + \frac{\partial q}{\partial z} = 0 \tag{7}$$

$$\frac{\partial q}{\partial t} + \frac{\partial}{\partial z}\left(\delta_1 \frac{q^2}{A}\right) + \frac{A}{p}\frac{\partial p}{\partial z} = Af_z + \frac{2\pi R}{\rho}\tau_w + \frac{\eta}{\rho}\frac{\partial^2 q}{\partial z^2} \tag{8}$$

being A(z, t) the lumen cross-sectional area, q(z, t) the average flow rate, p(z, t) the average pressure over the cross-section at a distance z from the inlet of the domain; f_z is the axial component of the body force, η is fluid dynamic viscosity, ρ is constant fluid density, t is the time, R is the lumen radius and z is the axial space coordinate [18]. In addition, τ_w is defined as the wall frictional force and can be estimated using different velocity profile functions: in the case of the modified flat velocity profile $\delta_1 = 1$, so $\tau_w = -\frac{3\eta}{R}\frac{q}{A}$, while for the parabolic velocity profile $\delta_1 = \frac{4}{3}$, so $\tau_w = -\frac{4\eta}{R}\frac{q}{A}$. Different is the case of the logarithmic velocity profile derived from Bessems et al. [21], which depends on three parameters, i.e. local flow rate (q), pressure gradient $\frac{\partial p}{\partial z}$ and Womersley number α (in this case δ_1 ranges from 1.058 to 1.065). The following figure (*Figure 8*) shows the three velocity profiles abovementioned at time t = 0.115 s and at location z/L = 0.5 of the aorta.

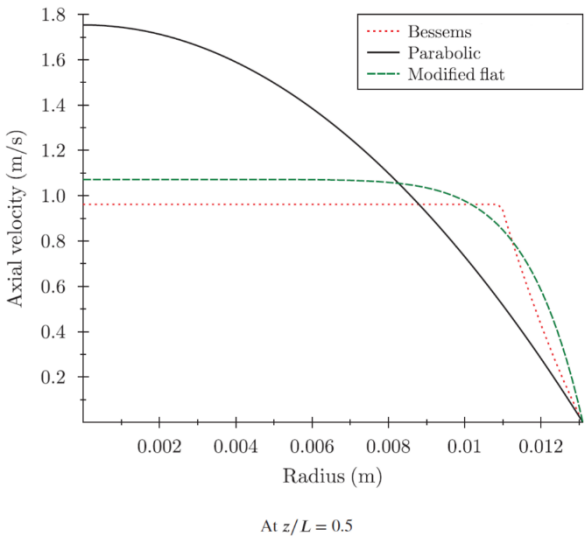

Figure 8: comparison of Bessems, modified flat and parabolic velocity profiles at z/L = 0.5 of aorta at t = 0.115 s. [18]

As reported by Hasan et al. [18], in order to solve the system of Navier-Stokes equations presented earlier, it is needed one more equation in the form of relation between stress and strain for artery wall: first linear elastic, then linear viscoelastic models and their constitutive equations are

considered with the aim of modelling the mechanical behaviour of the artery's wall. In the linear elastic model, the artery is considered to be made up of isotropic and homogeneous material and the relationship between hoop stress $\sigma_{\theta\theta}$ and strain $\varepsilon_{\theta\theta}$ is based on the assumptions that there is no axial deformation ($\varepsilon_{zz} \approx 0$) and the radial normal stress is negligible ($\sigma_{rr} << \sigma_{\theta\theta}$). The linear viscoelastic material model, instead, is a three-parameter based standard linear solid model (Zener model) involving two linear elastic springs and a dashpot [18]. In the latter case, the relationship between hoop stress and strain is more elaborate and includes parameters such as τ_σ and τ_ε, respectively strain relaxation time and stress relaxation time.

Moreover, the 1D wave propagation model is completed by adding specific boundary and initial conditions: at the inlet of the domain, a known flow rate (*Figure 9*) is prescribed, while the outlet boundary condition is coupled with a three element based zero-dimensional Windkessel model to account for the effect of downstream part of the arterial network. Windkessel model consists of two resistance R_1, R_2 and compliance C.

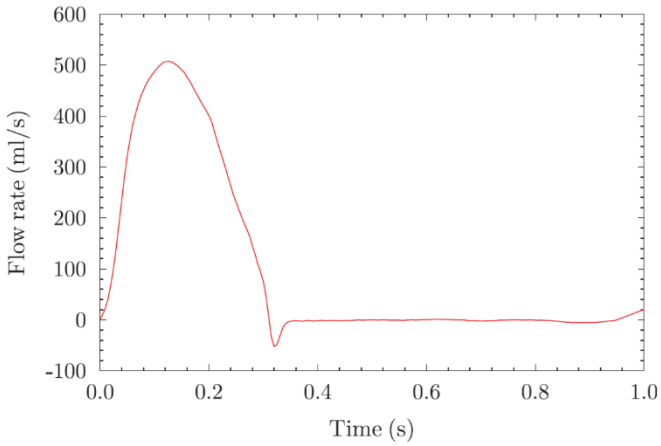

Figure 9: flow rate at the inlet of Aorta for input parameters mentioned in paragraph 3.2.2. [18]

The flow rate and pressure relationship at the outlet of the domain is given by the following equation

$$q\left(1+\frac{R_1}{R_2}\right)+CR_1\frac{\partial q}{\partial t}=\frac{p-p_{out}}{R_2}+C\frac{\partial p}{\partial t} \qquad (9)$$

and initial conditions are set as follows:

$$q(z,0)=0,\ \ A(z,0)=A_d,\ \ p(z,0)=p_d$$

being p_d the diastolic pressure and A_d the area of the Aorta at pressure p_d.

3.2.2 SIMULATIONS AND RESULTS

As previously mentioned by Hasan et al. [18], simulations are carried out in two different cases: aorta modeled as a single arterial segment and considered as a complete arterial network. Focusing on the first case (a single arterial segment is discretized in space using ten quadratic finite elements), aorta is represented as a straight cylindrical vessel of length L = 24.137 cm, diameter D = 2.4 cm at

the diastolic pressure p_d = 9.5 kPa and a constant wall thickness h = 1.2 mm and both elastic and viscoelastic constitutive laws are used to model the artery. The main parameters regarding blood and wall properties and Windkessel parameters used for the numerical simulations are given in *Table 3*.

Wall (viscoelastic material) properties			
E	E_v	β_v	μ
400×10^3 N/m^2	223.5×10^3 N/m^2	40×10^4 N/m^2	0.5
Wall (elastic material) properties[2,11]			
E			μ
400×10^3 N/m^2			0.5
Blood properties[11]			
ρ			η
1,060 kg/m^3			4×10^{-3} N s/m^2
Windkessel parameters[11]			
R_1	R_2	C	
1.1752×10^7 Pa s m^{-3}	1.1167×10^8 Pa s m^{-3}	1.0163×10^{-8} Pa^{-1} m^3	

Table 3: blood, artery properties and Windkessel parameters used in aorta simulation; E_v and β_v are respectively the elastic modulus of the springs belonging to the viscoelastic part of the Zener model and the coefficient of viscosity of the dashpot. [18]

Pressure and flow rate curves, obtained as the result of the simulations using linear elastic model for the three velocity profiles, are then compared with 3D results by Xiao et al. [26], obviously more precise, arising from a more complex and a higher-order model. The confrontation of results for the case of Bessems [21], modified flat and parabolic profiles and Xiao's 3D analysis in different locations of aorta is shown in *Figure 10* for the elastic model and in *Figure 11* for the viscoelastic one.

As stated by Hasan et al. [18], in the case of the linear elastic model, the relative errors in terms of pressure and flow rate are calculated with respect to Xiao et al. [26] 3D results: the error associated with the Bessems velocity profile is lower as compared to errors associated with modified flat and parabolic velocity profile functions; the smaller error prediction can be attributed to the flow dynamics considered by Bessems et al. [21] in the derivation of velocity profile, resulting into better estimation of convection (δ_1) and viscous terms [18]. Furthermore, it can also be concluded that the assumption of Bessems velocity profile is more accurate as opposed to parabolic velocity, which is less accurate. In both elastic and viscoelastic models, differences in the average relative error associated with flow rate/pressure prediction using the three different velocity profiles fall within 0.5% at all measuring locations (the maximum relative error is highest for parabolic velocity profile). It can also be inferred from *Figures 10* and *11* that the linear viscoelastic model predicts lower flow rate and pressure compared to the linear elastic model for the set of parameters used in the simulation. [18]

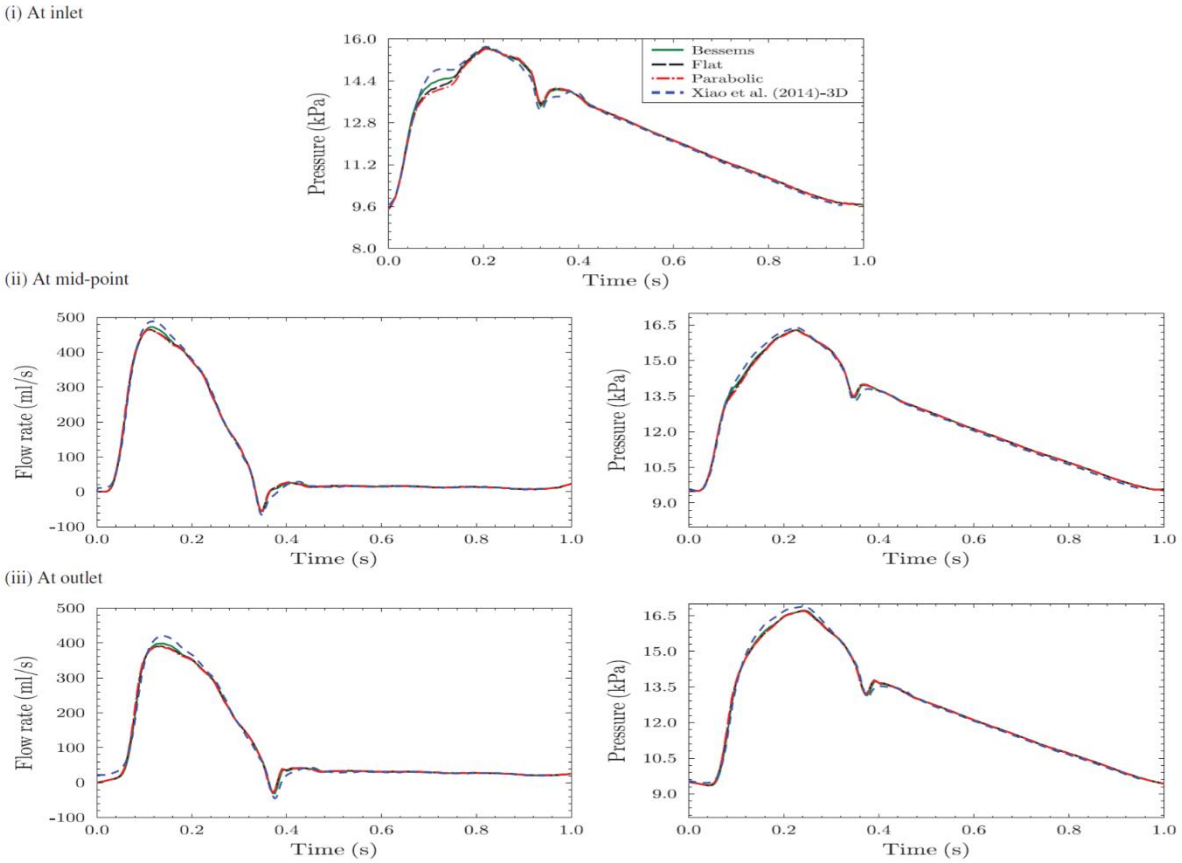

Figure 10: Comparison of results obtained at inlet, midpoint and outlet by using Bessems [21], modified flat and parabolic velocity profiles in case of elastic model of the arterial wall. [18]

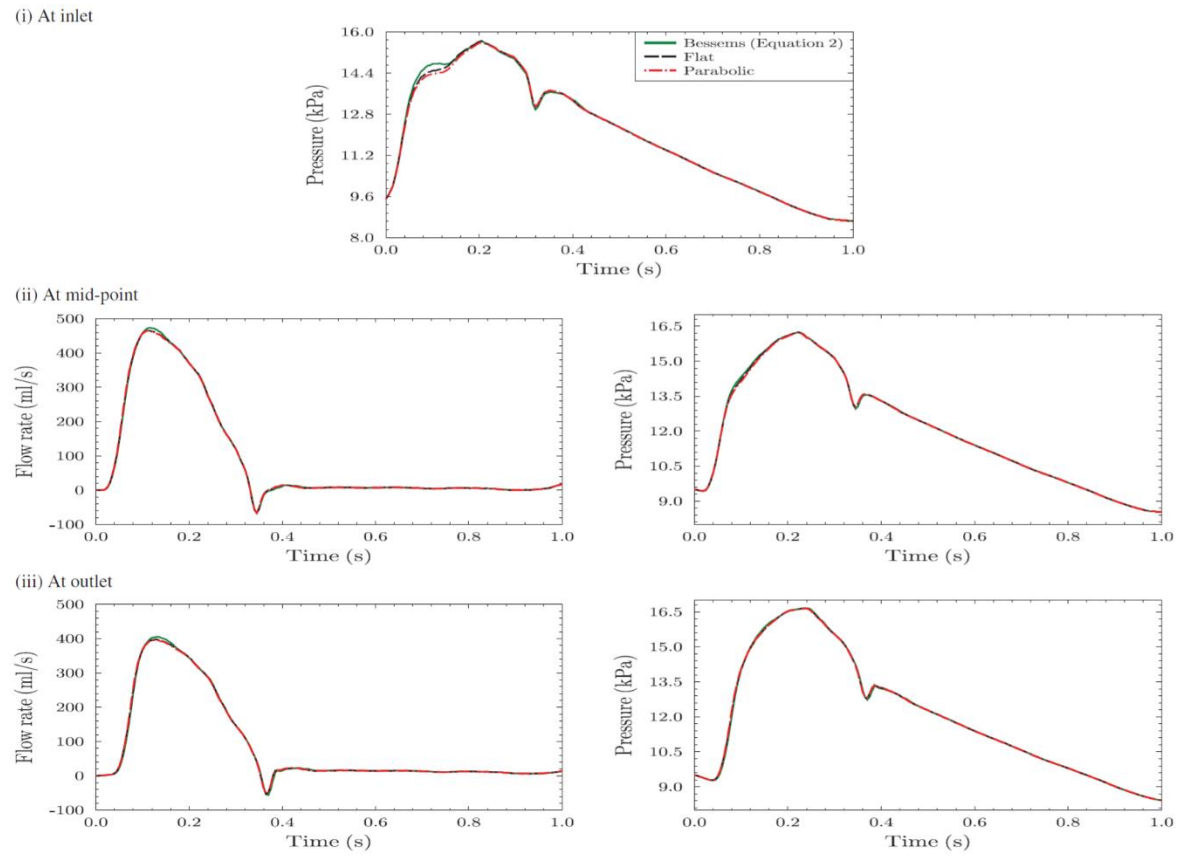

Figure 11: comparison of results obtained at inlet, midpoint and outlet by using Bessems [21], modified flat and parabolic velocity profiles in case of viscoelastic model of the arterial wall. [18]

Finally, the root mean square value, that is the difference in the pressure prediction between the material models, is greatest for Bessems profile and is smallest for the modified flat profile, while in the case of flow rate prediction, just the opposite trend is observed.

Regarding instead the second case proposed by Hasan et al. in [18], i.e. the simulation carried out in an arterial network, aorta is idealized as a complete network consisting of an aorta segment and its main branches, as shown in *Figure 12* [18].

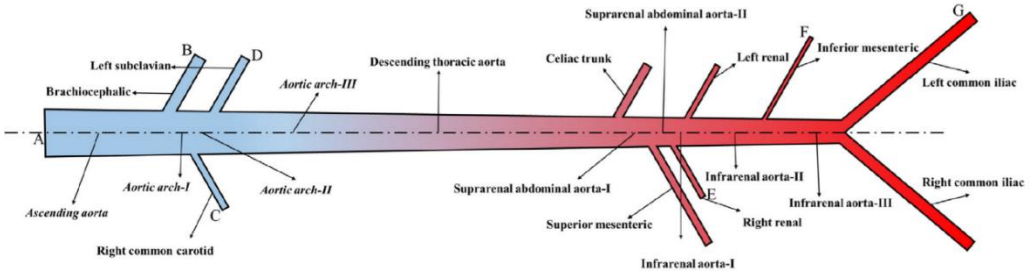

Figure 12: complete aorta network with 20 aorta segments and main branches. [18]

For the sake of simplicity, all branches are considered straight small cylinders and curvatures of the arteries are neglected; the arterial network is modeled using 200 finite elements and 420 nodes (10 one dimensional elements per branch) [18]. As it has already been done in the first case previously analysed, flow rate and pressure variation with time at different locations predicted using Bessems, modified flat and parabolic velocity profiles are compared with 3D results of Xiao et al. [26] (in *Figure 13*) for the elastic arterial model. The flow characteristics

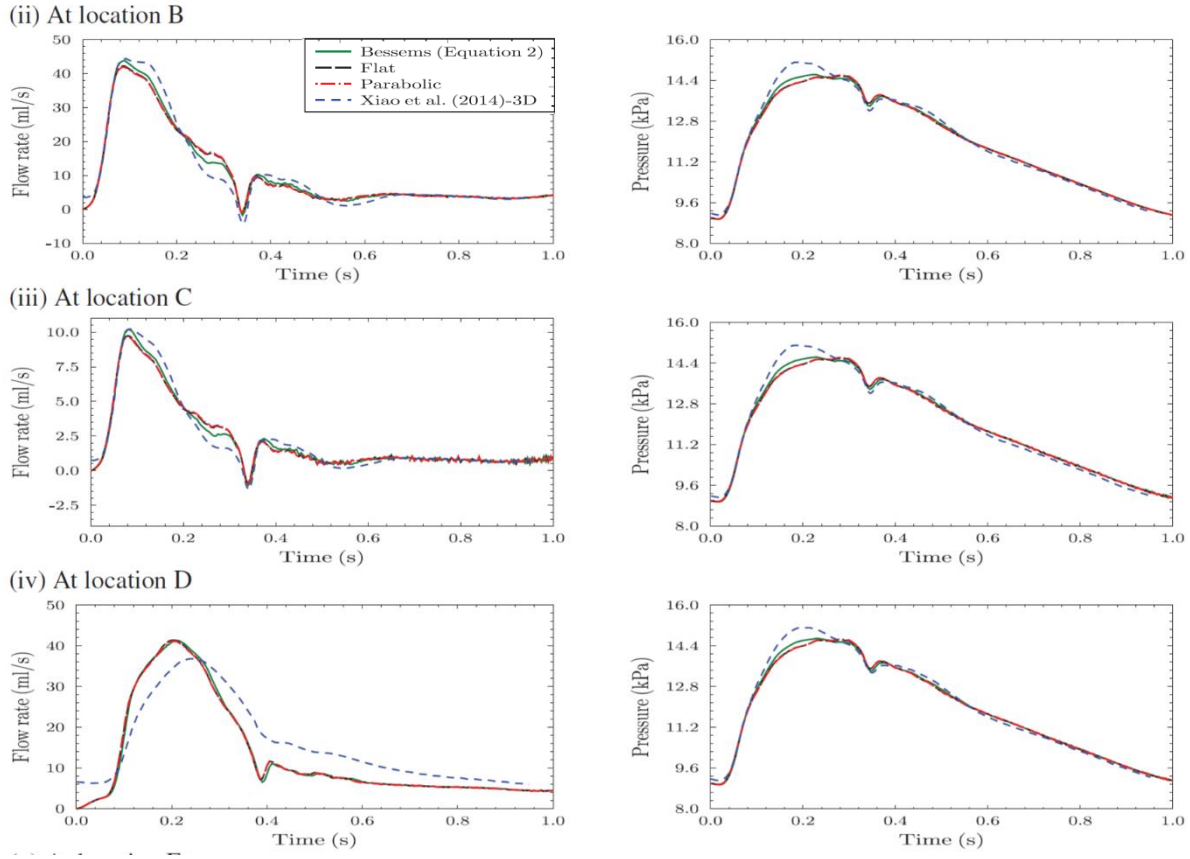

Figure 13: comparison of flow rate (left) and pressure distribution (right) at locations B, C, D of the arterial network modeled as elastic. [18]

prediction for the viscoelastic material model using Bessems, modified flat and parabolic velocity profiles are compared in *Figure 14*. Moreover, in the case of elastic arterial model, relative errors of pressure, and flow rate at different locations are calculated with respect to 3D results of Xiao et al. [26]: it is found that for most of the cases, the error associated with the Bessems velocity profile is lesser as compared to those associated with modified flat and parabolic velocity profile functions. Here too, smaller error prediction is attributed to flow dynamics considered by Bessems et al. [21] in the derivation of velocity profile, resulting in better estimation of convection (δ_1) and viscous terms. It is also noticed that both average and maximum errors in the flow rate prediction are significantly higher as compared to errors in the pressure prediction, due to the initial conditions imposed. [18]

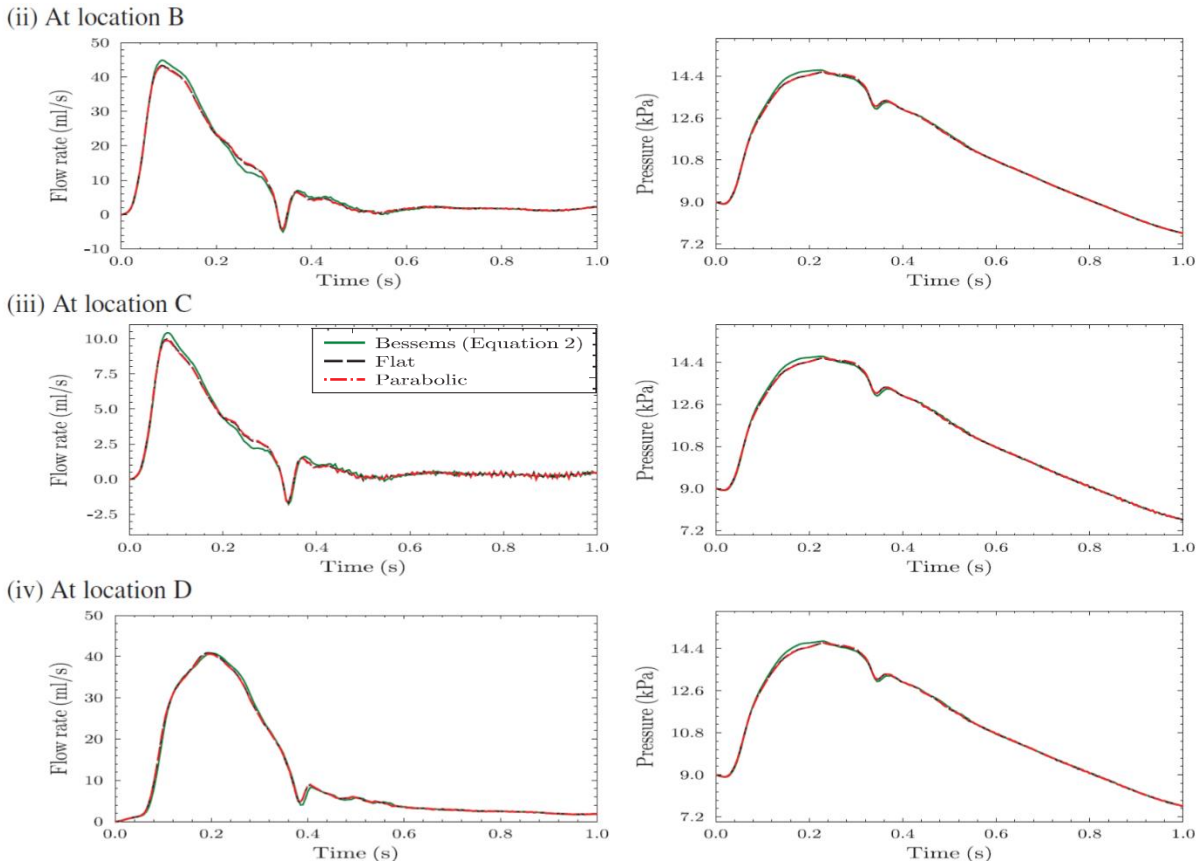

Figure 14: comparison of flow rate (Left) and pressure distribution (right) at locations B, C, D of the arterial network modeled as viscoelastic. [18]

Lastly, the linear viscoelastic model predicts lower flow rate and pressure as compared to the elastic model.

To summarize, as reported by Hasan et al. [18], 1D wave propagation model in time domain is used to numerically predict the flow behaviour and pressure distributions in the single aorta and aorta network, considering different cross-sectional velocity profiles. The flow characteristics predictions for the three different velocity profile functions are found to be quite close and coherent with a more

precise and complex simulation of a 3D model, introduced by Xiao et al. in [26]. It can be seen a good agreement between the 1D and 3D models in the elastic case, especially during diastole, while the greater error in systole is due to the inability to account for secondary flow features, to the one dimensional modelling of arterial vessels (approximated as small cylinders and curvatures are neglected) and, particularly, due to the fixed velocity profile used (in order to achieve a better compliance compared to 3D models, the 1D formulation could incorporate space-varying and time-varying velocity profiles [26]). In addition, the results achieved are remarkably dependent on the constitutive model used for approximating arteries' mechanical behaviour, namely linear elastic and linear viscoelastic: in case of elastic arterial wall model, wave speed is found to be greater than that for the viscoelastic case. Furthermore, time gap in the arrival of the waves at different locations of the domain is clearly noticeable in the results and flow rate and mean pressure predicted by viscoelastic model are less as compared to the elastic model. As concluded by Hasan et al. [18], results of linear elastic model using Bessems logarithmic velocity profile are found to be in better agreement with the 3D results of Xiao et al. [26] as compared to modified flat and parabolic velocity profiles. [18]

Thus, it can be asserted that the 1D model presented by Hasan et al. [18] gives a reasonable representation of the 3-D system in terms of the global behaviour of the spatially averaged pressure and flow waveforms: this can lead this one dimensional model to be used to reproduce clinical measurements and to conduce sensitivity studies under different hemodynamic conditions, in order to gain an understanding of the behaviour of the arterial system. [26]

3.3 REDUCED ORDER MODELING OF BLOOD FLOW FOR THE EVALUATION OF CORONARY ARTERY DISEASE

Coronary artery disease, or simply CAD, is one of the most severe blood flow related diseases which causes a great percentage of fatalities worldwide every year, therefore it is a focal spot in the medical field and in ROMs development. Many times, CAD can occur in the form of arterial stenosis, that is to say an abnormal narrowing of the vessel that can cause, in this case, reduced blood flow to the region of the myocardium [27]. As stated by Buoso et al. [27], clinically, the functional severity of the stenosis can be quantified with the fractional flow reserve (FFR) index: FFR is calculated as the ratio between the blood pressure distal to a stenosis and the aortic blood pressure, both of which are invasively measured under hyperaemic conditions using a pressure wire catheter. Despite the effectiveness of this method, invasive analysis may overestimate the lesion severity, increasing the pressure drop in the area of interest [27].

Among the numerous computational haemodynamic models (usually 1D models) proposed to assess coronary stenosis severity (FFR derivation is highly expensive in the matter of computational cost and time), a different one was introduced by Buoso et al. [27]: aiming at predicting the pressure drop along a stenosed vessel, the model builds on the exact algebraic form of the unsteady incompressible Navier-Stokes equations and continuity equations used in the full-order model (FOM), thus creating a nonlinear ROM based on offline-online splitting of the computations. Furthermore, the hemodynamic equations are discretized with the finite volume (FV) method and the system dimensionality is reduced by projecting the FOM onto a subspace obtained from proper

orthogonal decomposition (POD) of a dataset of velocity and pressure fields. The algebraic operators of the equations in the ROM are then assembled efficiently with low computational cost in the online phase using the discrete empirical interpolation method (DEIM). [27] This is set to increase the rapidity of calculations, maintaining relative errors within the uncertainty limits of the invasive clinical measurements.

3.3.1 MODEL IMPLEMENTATION

As have already been mentioned, the method proposed consists in an offline-online splitting on the computations, as it can be observed in *Figure 15*.

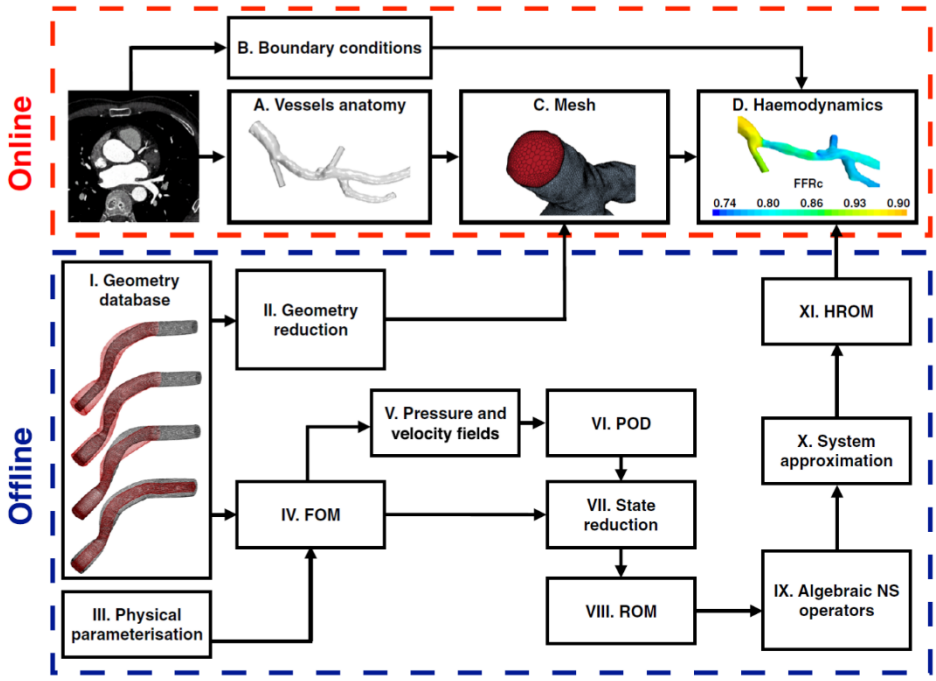

Figure 15: the online block (steps A to D) corresponds to the conventional calculation process using a full-order model. The offline block contains the steps used for the geometric parametrization and the creation of a reduced-order hemodynamic model. The two outputs of the offline block are the geometry reduction (II) and the HROM (XI), which are used in online steps C and D, respectively, for the calculation of subject-specific FFR. [27]

As reported by Buoso et al. in [27], the online process starts with the acquisition of images using computed tomography and the segmentation of the branches of interest (step A), then, a computational domain is created from the vessel lumen (C) and used for the discretization of the incompressible Navier-Stokes equations (a full order model (FOM) is obtained). The numerical procedure requires the coupling of the resulting system of equations with boundary conditions, which are derived from subject-specific non-invasive clinical images and measurements (B). In phase D, Navier-Stokes equations are solved and FFR computed [27].

The offline section starts from a database of geometries (I) that approximate the main features of coronary arteries (geometries are obtained from the deformation of a three-dimensional straight pipe with diameter d_0 = 4 mm and length L_0 = 40 mm, *Figure 16*). Applying DEIM to the vertex

coordinates of the domains, a set of geometrical bases is obtained (II): the latter, weighted by appropriate coefficients, can reconstruct the computational domain inside a given vessel, reducing the computational time of the step (C) in the online phase. [27]

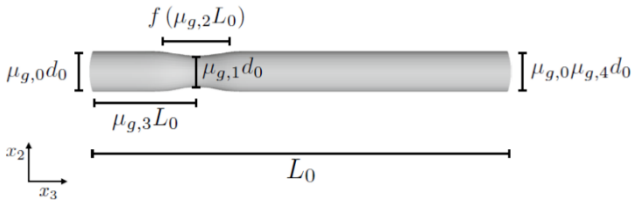

Figure 16: reference domain (representing a coronary artery branch) with added features (changes of the geometry due to stenosis and tapering): $\mu_{g,0}d_0$ is the inlet diameter, $\mu_{g,0}\mu_{g,4}d_0$ the outlet diameter, $\mu_{g,1}d_0$ the diameter of the stenosis throat, $\mu_{g,3}d_0$ the throat position on the x_3 axis, L_0 is the total length (constant for all geometries). The stenosis length is a function of $\mu_{g,2}L_0$. $\mu_{g,0}$ is the diameter scaling factor and $\mu_{g,1}$, $\mu_{g,2}$ and $\mu_{g,3}$ are the amplitude, length and throat position parameters of the bell-shaped restriction, respectively. [27]

Moreover, in the offline step III, the boundary conditions for blood vessels are parametrized imposing physiologic blood flow conditions by prescribing the inlet velocity profile (simulations are carried out using an axisymmetric parabolic inlet velocity profile). Subsequently, the geometric and physical parameters identified in steps I and III are used to create a predefined set of FOMs, obviously based on the parametrized unsteady Navier-Stokes equations (see *Paragraph 1.3*), to which are added boundary condition at the inlet (velocity profile imposition, as already said) and at the outlet (Cauchy stress tensor set to zero) of the domain. Then, the hemodynamic equations are discretized in both time and space using a FV solution strategy (IV), obtaining the corresponding velocity and pressure fields (V) [27]. As explained by Buoso et al. [27], proper orthogonal decomposition (POD) and discrete empirical interpolation method (DEIM) are employed in order to reduce the dimensionality of both geometric and hemodynamic descriptions: the first is used to construct the reduced bases for the velocity and the pressure fields, whose linear combination can reconstruct the original solutions. By imposing the orthogonality of the algebraic formulation of the FOM on the POD bases (Galerkin projection), the system's dimensionality of states can be reduced (VII). Thus, this leads to a proper reduced-order model with low dimensionality, referred to as ROM (VIII). However, the ROM still requires the calculation of all operators in the FOM ahead of their projection onto the POD bases. For this purpose, DEIM is used on FOM's matrices (X) in such a way as to enable the determination of an approximation of the algebraic description of the Navier-Stokes operators, which will allow their efficient assembly during the online solution process (XI). The ROM using the DEIM approximation to reconstruct the operators is referred to as hyper-reduced ROM (HROM): with this final ROM, the time to solution of subject-specific calculations will be reduced. [27]

3.3.2 RESULTS AND ANALYSIS

As stated by Buoso et al. [27], the geometry database has been populated with 100 different synthetic geometries by assigning values to the coefficients that appear in *Figure 16*, ranging from a minimum to a maximum value (*Table 4*).

μ_g	Parameter	Range		
		Min	Max	
$\mu_{g,0}$	Inlet diameter	2.0	6.0	mm
$\mu_{g,1}$	Stenosis severity	0.2	0.5	–
$\mu_{g,2}$	Stenosis length	0.5	1.0	10^{-4}
$\mu_{g,3}$	Stenosis position	0.37	0.63	–
$\mu_{g,4}$	Tapering	0.85	1.15	–

Table 4: parameters and their value ranges for the geometry database; are also indicated the geometric features they affect. [27]

Once defined the initial database, the geometric parametrization is carried out through the application of the discrete empirical interpolation method (DEIM) to 75 out of 100 geometries present within the database; chosen three values of tolerance ε (10^{-2}, 10^{-3} and 10^{-4}) for DEIM and their respective bases (3, 5 and 7 basis), the mean geometry of the vessel can be computed (*Figure 17a*) and obtained from the point-wise average of the coordinates of the domains in the dataset.

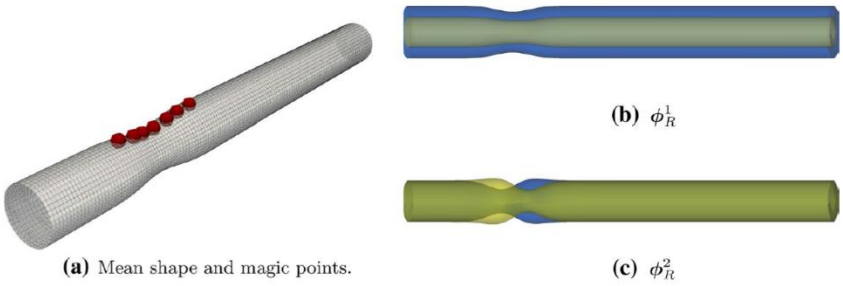

Figure 17: output of geometric parametrization. (a) mean shape and magic points (red spheres) for the case with $\varepsilon = 10^{-4}$, (b) first and (c) second reconstruction modes: the yellow shape corresponds to the minimum value of the reconstruction coefficient, the blue shape to the maximum value. [27]

Subsequently, for each of the defined training geometries, a constant parabolic inlet velocity profile is set with a mean velocity magnitude between 0.2 and 1.2 m/s (flow regimes with Reynolds numbers between 200 and 1200) and snapshots of pressure and velocity, obtained from FOMs, are stored. Afterwards, POD is applied to the calculation of velocity and pressure subspaces and ROM's constitutive matrices are solved, storing Navier-Stokes operators. Then, DEIM is applied to reconstruct the operators and a reduced mesh of the original domain is obtained: as stated by Buoso et al. [27], "since when using the HROM we are only required to assemble the algebraic NS operators for the cells of the reduced mesh, during the online phase we use the geometric parametrization to reconstruct the cells of the reduced mesh, decreasing the computational cost compared to the reconstruction of the full mesh". [27] In *Figure 18* is shown the reduced mesh for the computation of DEIM coefficients.

Figure 18: reduced mesh for Navier-Stokes operators of the HROM. The panels represent the cells of the full mesh (red elements) required for the calculation of the coefficients used to impose the interpolation constraints on DEIM (convective, Laplacian, pressure-gradient and pressure-Laplacian operators). The background geometry refers to the mean geometry obtained from the geometric parametrization (transparent background, see Figure 17). [27]

Ultimately, HROM has been employed to pursue the purpose of Buoso's study, i.e. the prediction of the pressure drop in the geometries of the database for selected inlet flow velocities [27].

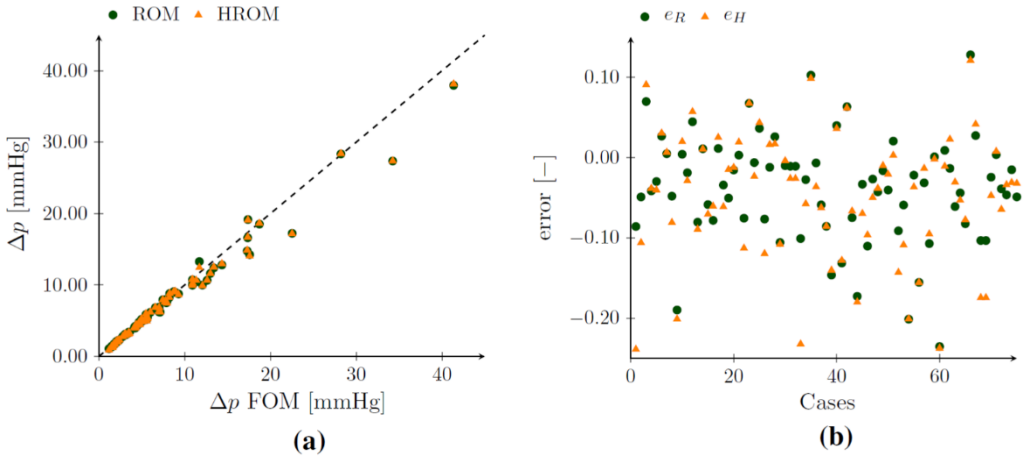

Figure 19: comparison of time averaged pressure drop predictions from FOM, ROM and HROM for the training set. (a) compares the pressure drop determined with the FOM (horizontal axis) to that calculated with the ROM (green dots) and the HROM (orange triangles), while (b) shows the relative errors in the pressure predictions: e_R (green dots) refers to the relative error between FOM and ROM, while e_H (orange triangles) to the relative error between FOM and HROM. [27]

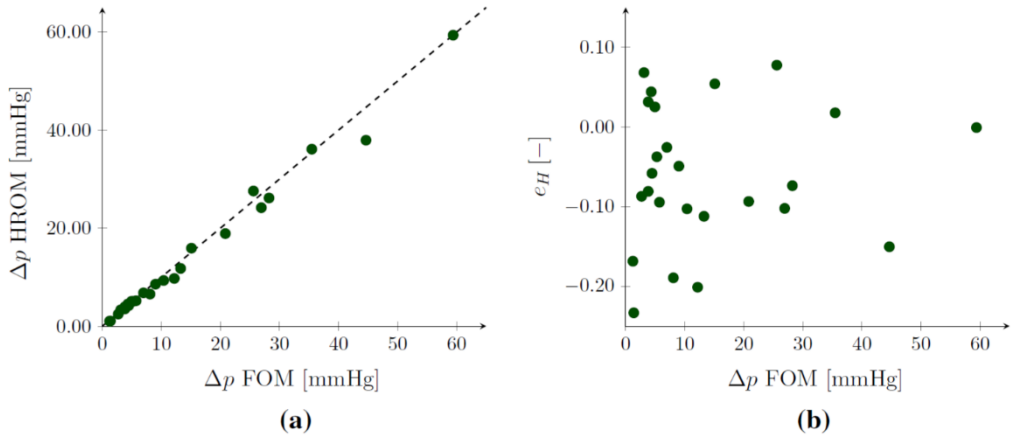

Figure 20: comparison of time averaged pressure drop predictions from FOM and HROM for the 25 test cases. (a) compares the pressure drop from the FOM (horizontal axis) to that calculated with the HROM, while b shows the relative errors in the pressure predictions between FOM and HROM as function of the pressure drop. [27]

Figures 19 and *20* show the comparison between FOM, ROM and HROM in the context of the calculation of the pressure drop in the stenosed artery vessel, also highlighting the relative errors in the pressure prediction in order to evaluate the uncertainties introduced during the Galerkin projection and the reconstruction of the operators using DEIM. Furthermore, Buoso et al. in [27] present the time-averaged velocity magnitude and pressure fields within the stenosed in the case of a section-averaged inlet velocity equal to 0.34 m/s, which is shown in *Figure 21*.

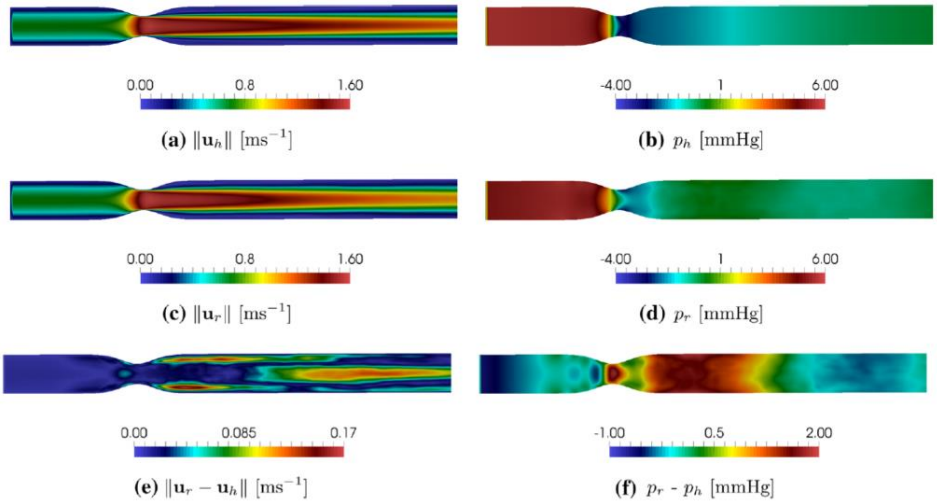

Figure 19: contours of time-averaged velocity (left panels) and pressure fields (right panels) for the case described by the parameters $\mu_{g,0}$ = 3.4 mm, $\mu_{g,1}$ = 0.48 , $\mu_{g,2}$ = 1.1 × 10^{-4} , $\mu_{g,3}$ = 0.47 , $\mu_{g,4}$ = 0.97 and μ_p = 0.34 m/s. The time-averaged pressure drops predicted by FOM and HROM are 5.69 mmHg and 5.59 mmHg, respectively. [27]

In *Figure 21*, panels (a) and (b) are respectively the velocity magnitude, $\|\mathbf{u}_h\|$, and pressure, p_h, predictions from the FOM, while (c) and (d) are the reconstructed velocity magnitude field, $\|\mathbf{u}_r\|$, and pressure, p_r , predictions from the HROM. Finally, panels (e) and (f) illustrate the absolute error in velocity and pressure of the HROM with respect to the FOM, showing the magnitude of velocity difference $\|\mathbf{u}_r - \mathbf{u}_h\|$ and difference in pressure $p_r - p_h$ [27]. Additionally, it can be brought to attention that there is a region downstream the stenosis characterised by negative pressure values (with the increasing of Reynolds number and the variations of geometrical parameters, this region grows in extension, as it can be seen in *Figure 22*): it is recalled that at the outlet of the domain pressure values are set to zero, thus after the stenosis a partial recovery of the pressure occurs.

Figure 20: reconstructed velocity magnitude field, $\|\mathbf{u}_r\|$, and pressure, p_r, predictions from the HROM for an inlet velocity of 1.05 m/s, $\mu_{g,0}$ = 3.0 mm, $\mu_{g,1}$ = 0.48, $\mu_{g,2}$ = 0.75 × 10^{-4}, $\mu_{g,3}$ = 0.04, $\mu_{g,4}$ = 0.93 and μ_p = 1.05 m/s. With respect to Figure 21, Reynolds number in the vessel is much higher and transition from laminar to turbulent flow can be seen. [27]

As stated by Buoso et al. [27], in the case presented in *Figure 21*, the prediction error e_H is 0.1 mmHg (2%) and the maximum error in the pressure field reconstruction is approximately 30%, while, as far as *Figure 22* is concerned, the time-averaged pressure drops predicted by FOM and HROM are 41.74 mmHg and 38.68 mmHg respectively, thus e_H is approximately 3 mmHg (8%) and the maximum error in the pressure field reconstruction is about 10%. The errors observed between FOM and ROMs are linked to the complexity of the flow structures, as illustrated in *Figures 21* and *22*: moreover, it is shown that the prediction errors in the pressure drop, e_H, is lower than the local maximum errors in the pressure fields, indicating that the output variable of interest is better approximated by the HROM than the full field [27].

Going back to *Figure 19*, it can be seen that the maximum prediction errors e_R and e_H are very close, indicating negligible additional errors in the HROM introduced by the approximation of the Navier-Stokes operators with DEIM. Generally, ROM and HROM tend to underestimate the pressure drop, maybe because the smallest flow structures with POD basis are neglected as well as some of the inherent viscous dissipation. As asserted by Buoso et al. [27], the errors e_H for training and test sets are very similar (*Figures 19* and *20*), indicating that the model introduced could be used for making predictions for new cases not included in the training set; in addition, is important to highlight that the magnitude of these errors is within the range of those introduced by the catheter wire during invasive FFR measurements, thus showing the potential of the method for the generation of reduced-order models fast enough for pressure drop predictions for clinical applications [27]. From a clinical point of view, high prediction accuracy must be achieved in cases where the FFR value is in the range of 0.75–0.85, since 0.8. is commonly used as the threshold below which a stenosis is considered functionally significant, therefore the cases close to the FFR threshold value should receive a higher weight (in the model presented by Buoso et al. all snapshots have the same weight), increasing the accuracy of the prediction. [27]

In terms of computational cost, the reduced order model introduced in [27] implies a high speed up, especially in the context of mesh generation and haemodynamic calculations: with the conventional pipeline, mesh generation takes on average 2 s on a single CPU core, but only 0.19 s with the proposed geometric reconstruction through DEIM, providing a speedup of about a factor of 10; on the other hand, considering the computational time for the generation of the time-dependent operators and the solution of the system of equations, the FOM requires on average 2.5 s on a single core for each time step, while the ROM requires 0.11 s on average. This corresponds to a speedup of a factor of about 25. [27]

To summarize, Buoso et al. [27] introduced a methodology for generating a parametrized reduced-order model (HROM) to predict the pressure drop along a blood vessel, based on an offline-online splitting of the solution process combined with proper orthogonal decomposition (POD) and the discrete empirical interpolation method (DEIM), in order to reduce the computational cost associated with mesh generation and the solution of the hemodynamic equations. Numerical results show good overall accuracy of the HROM in predicting hemodynamic indices, and a great speedup compared to the full-order model. Finally, errors are lower than those incurred during invasive acquisitions of pressure drop across stenoses in coronary arteries, thus ensuring a possible application of the model in clinical setting aiming at evaluating the severity of coronary artery disease in a rapid, precise and non-invasive way.

CONCLUSIONS

The cardiovascular system consists in a series of vessels of different sizes, thickness and structural properties which branch and link up, introducing a great number of discontinuities that are difficult to model; moreover, as far as haemodynamics is concerned, Reynolds number varies considerably depending on the type of vessel and on physiological or pathological conditions of blood flow. Flow rate and pressure characteristics constantly change in correspondence of the numerous interfaces between vessels and have generally a pulsatile behaviour (it can also be pointed out the non-Newtonian nature of blood, which further complicates a highly precise analysis). Thus, as it has been widely highlighted throughout this thesis, the extremely elevated complexity of the cardiovascular system both in terms of spatial geometry and fluid dynamics, makes the use of reduced order models indispensable when faster and cheaper analysis are required. In fact, ROMs have strongly broken into clinical settings, where accurate computations may have to be performed in a short amount of time, in order to support decision making processes and to evaluate the severity of pathological condition in patients. Furthermore, we have said that the benefits of reduced order models primarily consist in computational cost and time reduction with respect to full order models (FOMs), being also able to preserve the accuracy and precision that characterize the latters. As shown in *Chapter 3* in the works of Civilla et al. [17], Hasan et al. [18] and Buoso et al. [27], the reduced order models proposed are generally in good agreement with output results derived from 3D models and FOMs already existing in literature, demonstrating that errors are restrained and thus validating these ROMs. Therefore, it surely cannot be questioned the fact that, thanks to ROMs, a great computational burden is relieved: focusing, for example, on the parametrized model proposed by Buoso et al. [27], it has been proven that the ROM ensures a huge speedup both in terms of domain parametrizing (mesh generation), with a factor of 10, and of haemodynamic equations solving, actually 25 times much faster than the full order model. Another fundamental advantage introduced by the model abovementioned regards the fact that errors derived from the splitting of the calculations, the application of proper orthogonal decomposition (POD) and discrete empirical interpolation method (DEIM) are even smaller than the ones introduced by in-vivo measurements. Thus, in this and other cases, the utility and the clinical importance of such a model is obvious and can be well on the way to replace expensive FOMs in the context of patient-specific analysis.

Needless to say, the accuracy of the reduced order models strongly depends on their dimension, giving the fact that some important hypothesis and simplifications are employed in the full order model approximation: for example, a 0D model is well suited for the representation of the global haemodynamics of the whole circulation, but fails at giving precise results when the study of blood flow is carried out in restricted domains (this models neglect important haemodynamic aspects, such as pulse wave propagation in arteries). Moreover, in the case of a 1D model, although giving more precise results in terms of pressure and flow rate waveforms in artery vessels than a 0D model, a velocity profile must always be set in order to carry out simulations: this, obviously, constitutes a source of error that cannot be neglected when precise results are needed and the entity of the error is related to the type of velocity profile and structural vessel wall model chosen. For example, when modeling blood flow through aorta, Hasan et al. [18] compared the effect of three different profiles on the flow characteristics, concluding that a parabolic profile, which is the most commonly used

in simulations, provides less accurate outputs than other profiles (the problem of finding the most suited velocity profile to the aim of the study opens up), although still giving a very useful and quick approximation that can be used for real time analysis in the place of the FOM.

As stated by Dal Santo et al. [12], several challenges remain open when dealing with cardiovascular applications of reduced order models, such as among others to find new approaches to address multiphysics and multiscale models, to find a solution to the nonlinearity and high sensitivity of the solutions with respect to parameter variations, which limit computational speedups and, finally, to achieve patient-specific models that can safely replace three dimensional imagine based computational fluid dynamic models (CFD), thus obtaining a large number of advantages from a preventive, diagnostic and operative point of view in clinical settings.

BIBLIOGRAPHY

[1] J.R. Levick. “An introduction to Cardiovascular physiology”. Butterworths,1991.

[2] J.G. Betts et al., “Anatomy & Physiology”. Openstax, 2013.

[3] Colciago, C., Deparis, S.; Quarteroni, A., “Comparisons between reduced order models and full 3D models for fluid–structure interaction problems in haemodynamics”. *J. Comput. Appl. Math.* 2014, *265*, 120–138.

[4] T.J. Pedley. “The fluid mechanics of large blood vessels”. Cambridge University Press, 1980.

[5] W.W. Nichols, M.F. O’Rourke, McDonald’s “Blood Flow in Arteries - Theoretical, Experimental and Clinical Principles”, Arnold, 1998.

[6] B.M. Koeppen and B.A. Stanton. Berne & Levy Physiology. 6th ed. Elsevier, 2009.

[7] C. K. Zarins, D. P. Giddens, B. Bharadvaj, V. S. Sottiurai, R. F. Mabon, and S. Glagov, “Carotid bifurcation atherosclerosis. Quantitative correlation of plaque localization with flow velocity profiles and wall shear stress”, Circ. Res., 53 (4) (1983), 502–514.

[8] C. Gallo, “A multiscale modelling of the cardiovascular fluid dynamics for clinical and space applications”, 2021.

[9] R. Arina, “Fondamenti di aerodinamica”, Seconda edizione, Levrotto&Bella, Torino, 2015.

[10] Y. Shi, P. Lawford, and R. Hose. “Review of zero-D and 1-D models of blood flow in the cardiovascular system”. In: Biomedical Engineering Online 10 (2011), p. 33. doi: 10.1186/1475-925X-10-33.

[11] Benner, P., Gugercin, S. and Willcox, K. 2015. “A Survey of Projection-Based Model Reduction Methods for Parametric Dynamical Systems”. SIAM Review 57(4): 483–531.

[12] Dal Santo, N., Manzoni, A., Pagani, S., & Quarteroni, A. (2020). “Reduced-order modeling for applications to the cardiovascular system”. *Applications* (pp. 251-278) doi:10.1515/9783110499001-008

[13] C. J. G. Rojas, A. Dengel, and M. D. Ribeiro. “Reduced-order model for fluid flows via neural ordinary differential equations”. arXiv preprint arXiv:2102.02248, 2021.

[14] C.A. Taylor and C.A. Figueroa. “Patient-specific modeling of cardiovascular mechanics”. In: Annual Review of Biomedical Engineering 11 (2009), pp. 109–134. doi: 10.1146/annurev.bioeng.10.061807.160521.

[15] N. Stergiopulos, D.F. Young, and T.R. Rogge. “Computer simulation of arterial flow with applications to arterial and aortic stenoses”. In: Journal of Biomechanics 25 (1992), pp. 1477–1488. doi: 10.1016/0021-9290(92).

[16] O. Frank. “Die Grundform des Arteriellen Pulses”. In: Zeitschrift für Biologie 37 (1899), pp. 483–526.

[17] Civilla, L., Sbrollini, A., Burattini, L., & Morettini, M. (2021). “An integrated lumped-parameter model of the cardiovascular system for the simulation of acute ischemic stroke: Description of instantaneous changes in hemodynamics”. *Mathematical Biosciences and Engineering, 18*(4), 3993-4010. doi:10.3934/mbe.2021200

[18] Hasan M, Patel BP, Pradyumna S. Influence of cross-sectional velocity profile on flow characteristics of arterial wall modeled as elastic and viscoelastic material. Int J Numer Meth Biomed Engng. 2021; 37:e3454. https://doi-org.ezproxy.biblio.polito.it/10.1002/cnm.3454

[19] Formaggia L, Lamponi D, Tuveri M, Veneziani A. Numerical modeling of 1D arterial networks coupled with a lumped parameters description of the heart. Comput Methods Biomech Biomed Eng. 2006;9(5):273-288.

[20] Steele BN, Valdez-Jasso D, Haider MA, Olufsen MS. Predicting arterial flow and pressure dynamics using a 1D fluid dynamics model with a viscoelastic wall. SIAM J Appl Math. 2011;71(4):1123-1143.

[21] Bessems D, Rutten M, Van De Vosse F. “A wave propagation model of blood flow in large vessels using an approximate velocity profile function”. J Fluid Mech. 2007;580:145-168.

[22] M. Mirramezani, S.C. Shadden, “A distributed lumped parameter model of blood flow”, Ann. Biomed. Eng. 48 (12) (2020) 2870–2886, http://dx.doi.org/10.1007/s10439-020-02545-6.

[23] M. Rafieian-Kopaei, M. Setorki, M. Doudi, A. Baradaran, H. Nasri, “Atherosclerosis: process, indicators, risk factors and new hopes”, Int. J. Prev. Med., 5 (2014), 927–946.

[24] T. Korakianitis, Y. Shi, “Numerical simulation of cardiovascular dynamics with healthy and diseased heart valves”, J. Biomech., 39 (2006), 1964–1982.

[25] N. Stergiopulos, B. E. Westerhof, N. Westerhof, “Total arterial inertance as the fourth element of the windkessel model”, Am. J. Physiol., 276 (1999), H81–H88.

[26] Xiao N, Alastruey J, Alberto FC., “A systematic comparison between 1-D and 3-D hemodynamics in compliant arterial models”. Int J Numer Methods Biomed Eng. 2014;30(2):204-231.

[27] Stefano Buoso, Andrea Manzoni, Hatem Alkadhi, André Plass, Alfio Quarteroni, Vartan Kurtcuoglu, “Reduced-order modeling of blood flow for noninvasive functional evaluation of coronary artery disease”, Biomech. Model. Mechanobiol. 18 (6) (2019) 1867–1881.